J|A|C|S

A R T I C L E S

Mapping the Potential Energy Surface of the Tolylcarbene Rearrangement in the Inner Phase of a Hemicarcerand

Jean-Luc Kerdelhué, Kevin J. Langenwalter, and Ralf Warmuth*

Contribution from the Department of Chemistry, Kansas State University, Manhattan, Kansas 66506-3701

Received July 24, 2002 ; E-mail: warmuth@ksu.edu

Abstract: Photolysis of *p*-tolyldiazirine (**6**) in the inner phase of a hemicarcerand with four butane-1,4-dioxy linker groups (**5**) in $C_6D_5CD_3$ at 77 K yields the 5-methylcycloheptatetraene hemicarceplex **5⊙3b** in 41% together with innermolecular reaction products resulting from an insertion of transient *p*-tolylcarbene (**1b**) into an acetal C−H or linker C−O bond of **5** and from the addition of **1b** to an aryl unit of **5**. The yield of incarcerated **3b** increased up to 67% if **6** is photolyzed inside a hemicarcerand with deuterated spanners and butane-1,4-dioxy linker groups (d_{48}-**5**). Hemicarceplex **5⊙3b** is not formed if the photolysis is carried out in $CDCl_3$. Incarcerated **3b** is stable at room temperature in the absence of oxygen and is characterized by 1D and 2D NMR spectroscopy. In the presence of oxygen, **3b** reacts quantitatively to yield toluene and CO_2. Upon heating solutions of d_{48}-**5⊙3b** in $C_6D_5CD_3$, **3b** rearranges to **1b** and *m*-tolylcarbene (**18**). Both tolylcarbenes immediately react with the surrounding host. From a product analysis and the measured rate constants for the thermal decomposition of d_{48}-**5⊙3b** in the temperature range 70−102 °C, the activation parameters for the **3b** to **1b** and **3b** to **18** rearrangements are calculated (**3b** to **1b**: $\Delta G_{373}^{\ddagger} = 27.3 \pm 1.4$ kcal/mol, $\Delta H_{373}^{\ddagger} = 26.4 \pm 1.0$ kcal/mol, $T\Delta S_{373}^{\ddagger} = -0.9 \pm 1.0$ kcal/mol; **3b** to **18**: $\Delta G_{373}^{\ddagger} = 27.8 \pm 1.4$ kcal/mol, $\Delta H_{373}^{\ddagger} = 19.7 \pm 1.0$ kcal/mol, $T\Delta S_{373}^{\ddagger} = 8.1 \pm 1.0$ kcal/mol). These values are compared with those calculated by Geise and Hadad at the B3LYP/6-311+G** level of theory (Geise, C. M.; Hadad, C. M. *J. Org. Chem.* **2002**, *67*, 2532−2540). The slightly higher inner phase activation free energy of the **3b** to **18** rearrangement is explained through steric constraints imposed by the surrounding hemicarcerand on the transition state. The enthalpy−entropy compensation observed for the **3b** to **18** rearrangement is discussed and interpreted as a result of a hemicarcerand and solvent reorganization along the reaction coordinate. It is taken as indirect evidence for the intermediacy of 2-methylbicyclo[4.1.0]hepta-2,4,6-triene in the **3b** to **18** rearrangement.

Introduction

Arylcarbenes undergo fascinating rearrangements.[1] At high temperature in the gas phase, phenylcarbene **1a** ring-expands to cycloheptatetraene **3a**[2] (Scheme 1). The elucidation of the mechanism of the rearrangement of **1a** and of related arylcarbenes has been a great challenge since its discovery more than 30 years ago.[2,3]

In 1970, Baron, Jones, Jr., and Gaspar showed that pyrolysis of all isomeric tolyldiazomethanes yielded benzocyclobutene and styrene, which they rationalized through reversible equilibria involving tolylcarbenes, methylbicyclo[4.1.0]hepta-2,4,6-trienes, and methylcycloheptatrienylidenes (the π-mechanism) (Scheme 2).[4]
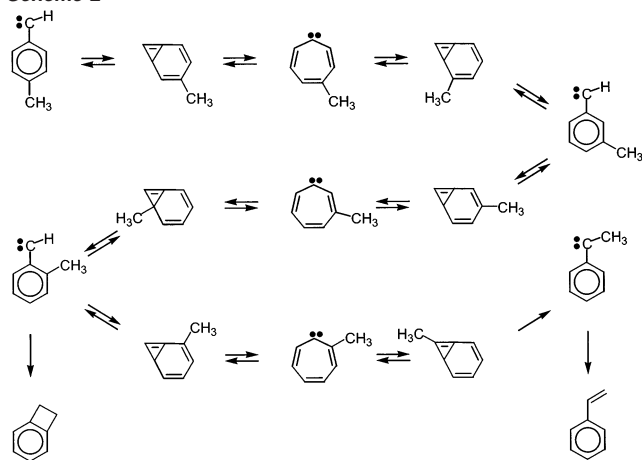
Scheme 1
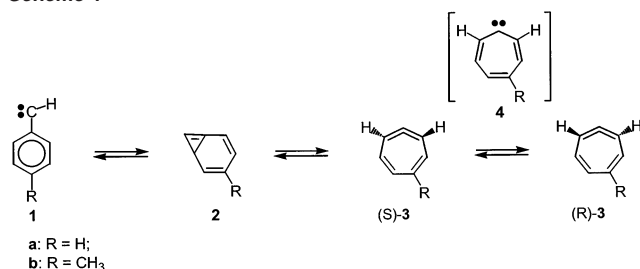
The identity of some of these postulated intermediates has been established spectroscopically in low-temperature matrixes.[5,6] Chapman and co-workers photolyzed all isomeric tolyldiazomethanes in argon at 10 K to produce the correspond-

(1) For reviews, see: (a) Moss, R. A.; Jones, M., Jr. *Reactive Intermediates*; John Wiley & Sons: New York, 1985; Vol. 3, p 91. (b) Wentrup, C. *Reactive Molecules*; John Wiley & Sons: New York, 1984; p 162. (c) Gaspar, P. P.; Hsu, J.-P.; Chari, S.; Jones, M., Jr. *Tetrahedron* **1985**, *41*, 1479. (d) Johnson, R. P. *Chem. Rev.* **1989**, *89*, 1111. (e) Platz, M. S. *Acc. Chem. Res.* **1995**, *28*, 487. (f) Karney, W. L.; Borden, W. T. In *Advances in Carbene Chemistry*; Brinker, U. H., Ed.; Elsevier: Amsterdam, 2001; Vol. 3, p 206.

(2) Joines, R. C.; Turner, A. B.; Jones, W. M. *J. Am. Chem. Soc.* **1969**, *91*, 7754.

(3) (a) Vander Stouw, G. G. Ph.D. Thesis, The Ohio State University, Columbus, OH, 1964. (b) Wentrup, C.; Wilczek, K. *Helv. Chim. Acta* **1970**, *53*, 1459.

(4) Baron, W. J.; Jones, M., Jr.; Gaspar, P. P. *J. Am. Chem. Soc.* **1970**, *92*, 4739.

(5) (a) Trozzolo, A. M.; Murray, R. W.; Wasserman, E. W. *J. Am. Chem. Soc.* **1962**, *84*, 4991. (b) West, P. R.; Chapman, O. L.; LeRoux, J.-P. *J. Am. Chem. Soc.* **1982**, *104*, 4, 1779. (c) McMahon, R. J.; Abelt, C. J.; Chapman, O. L.; Johnson, J. W.; Kreil, C. L.; LeRoux, J.-P.; Mooring, A. M.; West, P. R. *J. Am. Chem. Soc.* **1987**, *109*, 2456. (d) Chapman, O. L.; Abelt, C. J. *J. Org. Chem.* **1987**, *52*, 1218.

(6) Chapman, O. L.; Johnson, J. W.; McMahon, R. J.; West, P. R. *J. Am. Chem. Soc.* **1988**, *110*, 501.

Scheme 2

Scheme 3
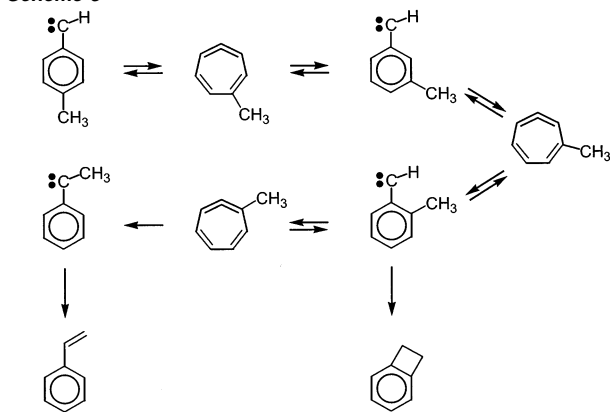
ing isomeric triplet tolyl carbenes, which upon further photolysis ring-expanded to methyl-substituted cycloheptatetraenes. The failure to observe evidence either for methylbicyclo[4.1.0]hepta-2,4,6-triene intermediates or for methylcycloheptatrienylidene intermediates in the photolysis or thermolysis of tolyldiazomethanes coupled with matrix isolation of the products led Chapman and co-workers to postulate a more simplified mechanism, which involves direct ring-expansions and -contractions of tolylcarbenes and methylcycloheptatetraenes (the σ-mechanism, Scheme 3).

In light of Chapman's experiments and recent high level ab initio calculations, several aspects of these rearrangements are still controversial and require an experimental verification and support:[7,8] (1) The singlet−triplet gap of **1**.[8a,9] (2) The role of **2** in these rearrangements. All ab initio calculations predict a phenylcarbene ring-expansion via the π-mechanism and **2** as an intermediate.[7,8b] This contradicts Chapman's matrix isolation studies, which gave no indication for **2**.[5b,c] Spectroscopic evidence for a bicyclo[4.1.0]hepta-2,4,6-triene intermediate has

Scheme 4
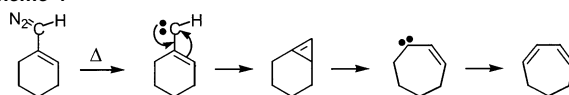
only been provided in the related naphthylcarbene rearrangement.[10] However, the preferential formation of 1,3-cycloheptadiene rather than 1,2-cycloheptadiene in the pyrolysis of 1-cyclohexenyldiazomethane can be viewed as strong experimental support for the π-mechanism (Scheme 4).[11] (3) The origin of the different behavior of arylcarbenes and arylnitrenes.[1e,f,7d] Whereas arylnitrenes ring-expand efficiently in condensed phases at ambient temperature,[12] the ring-expansion of singlet arylcarbenes requires much higher temperature.[1c,2−4] (4) The potential energy surface for the interconversion of the four postulated intermediates.[7,8b] Especially, the electronic nature of the transition state **4** for the enantiomerization of **3** and the influence of the environment on the barrier height are very important for our understanding of this fundamental step of arylcarbene rearrangements and for the solution phase chemistry of **3** and **4**.[13]

Recently, we have demonstrated that the inner phase of a hemicarcerand can serve as an inert phase, in which activation barriers of rearrangements involving highly strained intermediates can be measured with high accuracy.[14−17] Photolysis of *p*-tolyldiazirine, incarcerated inside a chiral hemicarcerand, yielded a mixture of two diastereomeric 5-methylcycloheptatetarene hemicarceplexes, whose thermal interconversion via the enantiomerization of the guest could be followed by ^{1}H NMR spectroscopy.[14]

Here we report our results of a detailed investigation of the photochemical tolylcarbene rearrangement in the inner phase of hemicarcerand **5**. Through a combination of NMR spectroscopic and kinetic experiments, we address several aspects that are important to arylcarbene rearrangements and to host−guest chemistry: (a) the barrier for the 5-methylcycloheptatetraene to *m*- and *p*-tolylcarbene rearrangement, which is an important section on the C$_8$H$_8$ potential energy surface; (b) the role of the surrounding hemicarcerand on the dynamics of both inner phase rearrangements; and (c) we also provide further indirect evidence for the participation of methylbicyclo[4.1.0]hepta-2,4,6-trienes in the tolylcarbene rearrangement.[11]
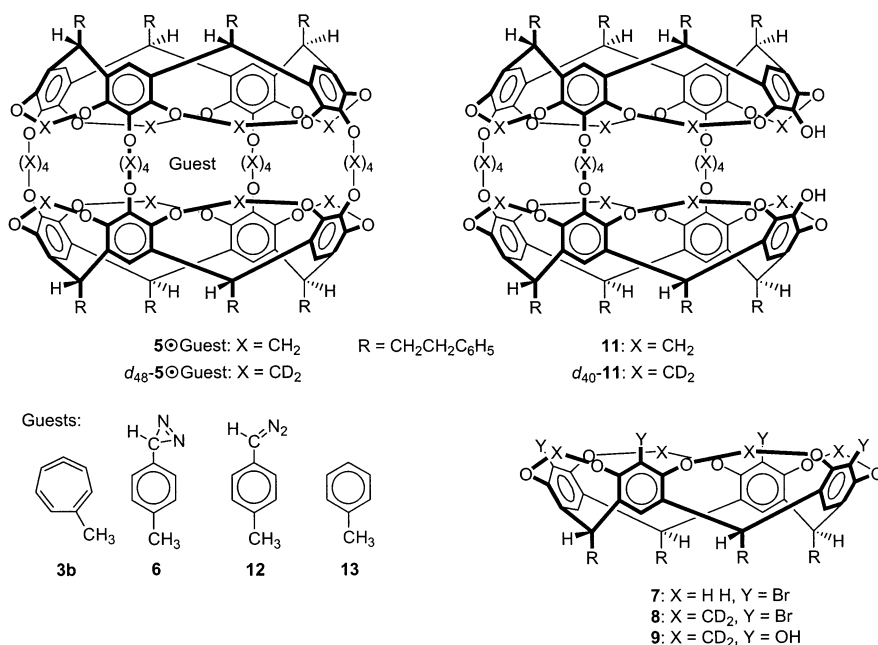
Results

Synthesis of Hemicarceplexes. We choose *p*-tolyldiazirine **6**[18] as the photochemical carbene precursor for our investigation
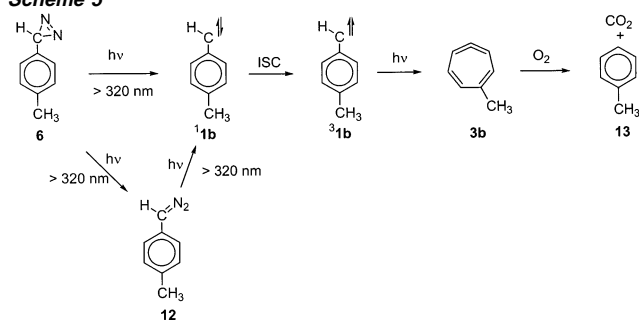
(7) (a) Matzinger, S.; Bally, T.; Patterson, E. V.; McMahon, R. J. *J. Am. Chem. Soc.* **1996**, *118*, 1535. (b) Wong, M. W.; Wentrup, C. *J. Org. Chem.* **1996**, *61*, 7022. (c) Schreiner, P. R.; Karney, W. L.; Schleyer, P. v. R.; Borden, W. T.; Hamilton, T. P.; Schaefer, H. F., III *J. Org. Chem.* **1996**, *61*, 7030. (d) Karney, W. L.; Borden, W. T. *J. Am. Chem. Soc.* **1997**, *119*, 1378. (e) Cramer, C. J.; Dulles, F. J.; Falvey, D. E. *J. Am. Chem. Soc.* **1994**, *116*, 9787.
(8) (a) Geise, C. M.; Hadad, C. M. *J. Org. Chem.* **2000**, *65*, 8348. (b) Geise, C. M.; Hadad, C. M. *J. Org. Chem.* **2002**, *67*, 2532.
(9) (a) Admasu, A.; Gudmundsdóttir, A. D.; Platz, M. S. *J. Phys. Chem. A* **1997**, *101*, 3832. (b) Seburg, R. A.; Hill, B. T.; Squires, R. R. *J. Chem. Soc., Perkin Trans. 2* **1999**, 2249. (c) Mendez, F.; Garcia-Garibay, M. *J. Org. Chem.* **1999**, *64*, 7061.

(10) (a) West, P. R.; Mooring, A. M.; McMahon, R. J.; Chapman, O. L. *J. Org. Chem.* **1986**, *51*, 1316. (b) Albrecht, S. W.; McMahon, R. J. *J. Am. Chem. Soc.* **1993**, *115*, 855. (c) Bonvallet, P. A.; McMahon, R. J. *J. Am. Chem. Soc.* **1999**, *121*, 10496. (d) Rempala, P.; Sheridan, R. S. *J. Chem. Soc., Perkin Trans. 2* **1999**, 2257.
(11) Miller, P.; Gaspar, P. P. *J. Org. Chem.* **1991**, *56*, 5101.
(12) Gritsan, N. P.; Zhu, Z.; Hadad, C. M.; Platz, M. S. *J. Am. Chem. Soc.* **1999**, *121*, 1202.
(13) (a) Harris, J. W.; Jones, W. M. *J. Am. Chem. Soc.* **1982**, *104*, 7329. (b) Kirmse, W.; Loosen, K.; Sluma, H.-D. *J. Am. Chem. Soc.* **1981**, *103*, 5935. (c) Kirmse, W.; Sluma, H.-D. *J. Org. Chem.* **1988**, *53*, 763.
(14) Warmuth, R. *J. Am. Chem. Soc.* **2001**, *123*, 6955.
(15) (a) Warmuth, R.; Marvel, M. A. *Angew. Chem.* **2000**, *112*, 1168; *Angew. Chem., Int. Ed.* **2000**, *39*, 1117. (b) Warmuth, R.; Marvel, M. A. *Chem.-Eur. J.* **2001**, *7*, 1209. (c) Warmuth, R. *Eur. J. Org. Chem.* **2001**, 423.
(16) Cram, D. J.; Tanner, M. E.; Thomas, R. *Angew. Chem.* **1991**, *103*, 1048; *Angew. Chem., Int. Ed. Engl.* **1991**, *30*, 1024.
(17) (a) Warmuth, R. *Angew. Chem.* **1997**, *109*, 1406; *Angew. Chem., Int. Ed. Engl.* **1997**, *36*, 1347. (b) Warmuth, R. *J. Chem. Soc., Chem. Commun.* **1998**, 59.
(18) Smith, R. A. G.; Knowles, J. *J. Chem. Soc., Perkin Trans. 2* **1975**, 686.

Chart 1

5⊙Guest: X = CH₂   R = CH₂CH₂C₆H₅   **11**: X = CH₂
*d*₄₈-**5**⊙Guest: X = CD₂   *d*₄₀-**11**: X = CD₂

Guests:

3b   **6**   **12**   **13**

7: X = H H, Y = Br
8: X = CD₂, Y = Br
9: X = CD₂, Y = OH

Scheme 5

of the tolylcarbene rearrangement inside hemicarcerands **5** and *d*₄₈-**5**. Heating tetrabromoresorcinarene **7**[19] and an excess of CD₂Cl₂ and K₂CO₃ in DMF at 80−85 °C for 9 days afforded cavitand **8** (49% yield),[14] which was converted into cavitand **9** according to a procedure described by Cram and co-workers for the parent nondeuterated cavitand.[20] The reaction of **9** with 3.5 equiv of *d*₈-butane-1,4-diol dimesylate (*d*₈-**10**)[14] and excess Cs₂CO₃ in NMP afforded *d*₄₀-**11** in 36% yield.[14] The latter was reacted with *d*₈-**10** (8 equiv) and excess Cs₂CO₃ in HMPA in the presence of **6** for 5 days to yield *d*₄₈-**5**⊙**6** (60% yield). Application of the same procedure to **11** and **10** gave **5**⊙**6** in 36% yield (Chart 1).[21]

Photolysis of Incarcerated *p*-Tolyldiazirine 5⊙6 and *d*₄₈-5⊙6. We have investigated the photochemistry of **5**⊙**6** and *d*₄₈-**5**⊙**6** under various conditions (Scheme 5). Brief UV-irradiation (λ > 320 nm) of a degassed solution of **5**⊙**6** in CDCl₃ at room temperature afforded a new hemicarceplex in 81% yield (Figure 1a, b). We assign this new compound to the tolyldiazomethane hemicarceplex **5**⊙**12** on the basis of a similar observation in the photochemistry of incarcerated phenyldiazirine[15b] and a characteristic IR absorption at 2084 cm⁻¹ (2065 cm⁻¹ at 15 K
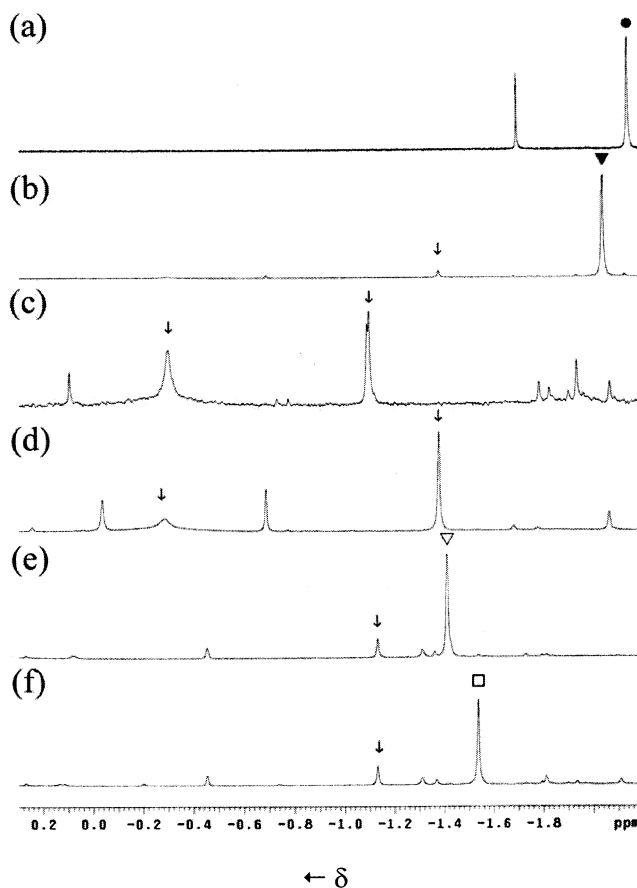
(19) Bryant, J. A.; Blanda, M. T.; Vincenti, M.; Cram, D. J. *J. Am. Chem. Soc.* **1991**, *113*, 2167.
(20) Cram, D. J.; Jaeger, R.; Deshayes, K. *J. Am. Chem. Soc.* **1993**, *115*, 10111.
(21) Warmuth, R.; Kerdelhué, J.-L.; Sánchez Carrera, S.; Langenwalter, K. J.; Brown, N. *Angew. Chem., Int. Ed.* **2002**, *41*, 96.

←δ

Figure 1. Partial ¹H NMR spectra (400 MHz, 22 °C) of a degassed solution of **5**⊙**6** (a−d) or *d*₄₈-**5**⊙**6** (e,f) in CDCl₃ (a−d) or C₆D₅CD₃ (e,f) before (a) or after UV irradiation (λ > 320 nm) for 30 s at 0 °C (b), 10 min at 0 °C (c), 2 h at 77 K (d−f). Spectrum f was recorded after the solution used for spectrum e was exposed to atmospheric oxygen for 30 min. Singlets assigned to the methyl protons of the *p*-tolyl group of **14**−**17** are indicated with arrows. The singlets assigned to the methyl protons of incarcerated **6**, **12**, **3b**, and toluene are marked with ●, ▼, ▽, and □, respectively.

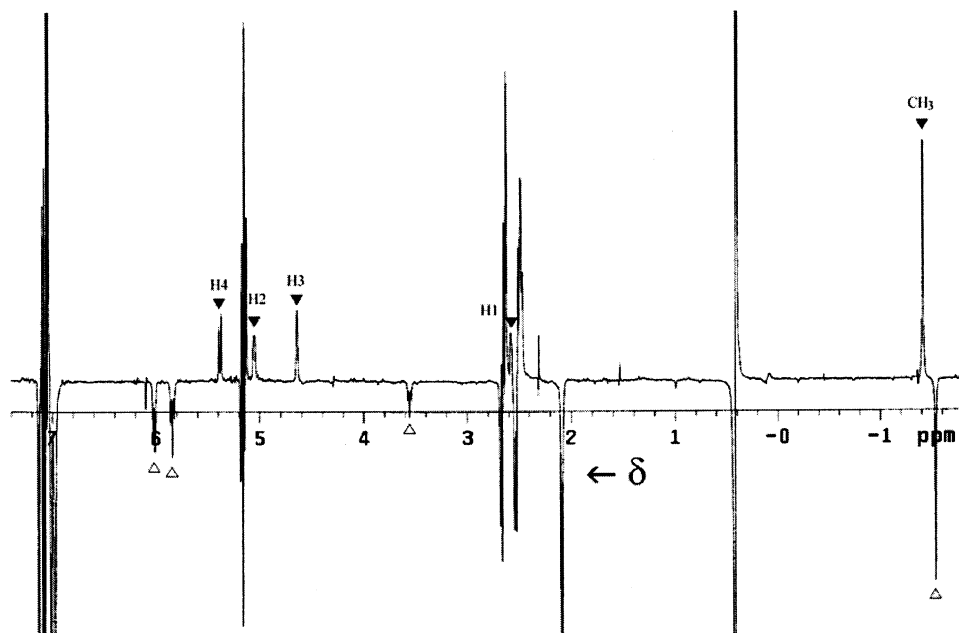in argon).[6] Further irradiation gave a complex product mixture resulting from the reaction of transient *p*-tolylcarbene with the

Figure 2. Spectral subtraction of the ^{1}H NMR spectra (400 MHz, 23 °C, C$_6$D$_5$CD$_3$) recorded before and after a solution containing approximately 60% of d_{48}-**5**⊙**3b** was exposed to oxygen for 30 min. Multiplets assigned to the protons of **3b** (upward pointing) and toluene (downward pointing) are marked with ▼ and △, respectively.

surrounding hemicarcerand (Figure 1c). Low-temperature pho-tolysis (77 K; $\lambda > 320$ nm) of **5**⊙**6** dissolved in CDCl$_3$ gave the same innermolecular[17b] insertion products in a different ratio as determined from the ^{1}H NMR spectrum of the reaction mixture (Figure 1d). In C$_6$D$_5$CD$_3$, which forms an organic glass at 77 K, the room temperature ^{1}H NMR spectrum showed the formation of a new hemicarceplex (41%) together with inner-molecular tolylcarbene insertion products. Prior investigation on the inner phase photochemistry of incarcerated phenyldi-azirine showed that under these conditions, transient singlet phenylcarbene partially undergoes intersystem crossing to triplet phenylcarbene. Excitation of the latter gives the ring-expanded cycloheptatetraene (**3a**).[15] On the basis of the photochemistry of incarcerated phenylcarbene, we assign the new hemicarceplex to **5**⊙**3b**, which forms via the photochemical ring-expansion of transient triplet tolylcarbene.[6] The yield of this new hemicar-ceplex increased to 55−67%, when we photolyzed **6** inside d_{48}-**5** (Figure 1e). Our assignment is further supported by the rapid reaction of **5**⊙**3b** with oxygen to give quantitatively CO$_2$ and **5**⊙toluene (Figure 1f).[14,15]

The formation of the latter hemicarceplex was confirmed by comparison with authentic sample prepared by heating **5** in toluene in a sealed tube (150 °C; 3 days).[22] Earlier, we observed this characteristic reaction for incarcerated cycloheptatetraene, which gave benzene and CO$_2$.[15a,b]

The room temperature ^{1}H NMR spectrum of d_{48}-**5**⊙**3b** obtained via spectral subtraction is shown in Figure 2. A combination of 2D NMR experiments (TOCSY, ROESY, and DQCOSY) allowed for the assignment of all guest protons. On the basis of the 2D-TOCSY (Figure 3) and the ROESY (t_{mix} = 600 ms) of a C$_6$D$_5$CD$_3$ solution containing 60% of d_{48}-**5**⊙**3b**, we assign protons H1−H5 to multiplets at δ 2.58 (d, 1H, J = 4.6 Hz), 5.06 (d, 1H, J = 4.6 Hz), 4.65 (sb, 1H), 5.37 (d, 1H,

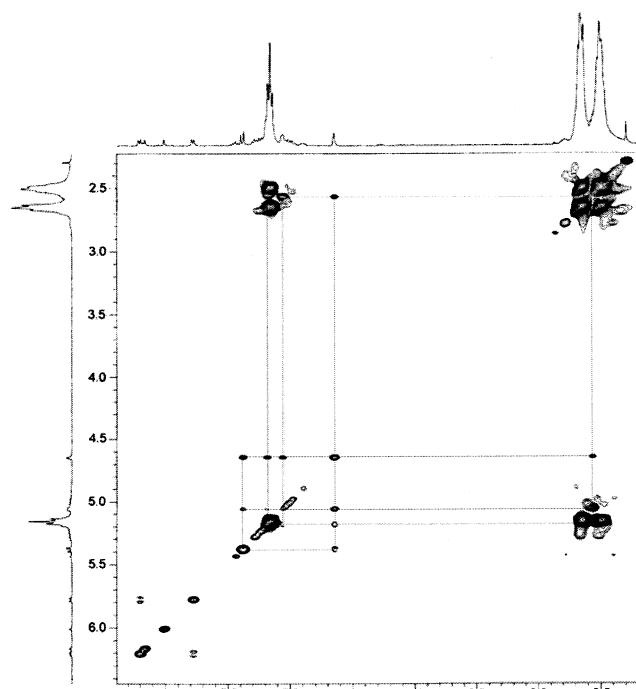(22) Makeiff, D. A.; Pope, D. J.; Sherman, J. C. *J. Am. Chem. Soc.* **2000**, *122*, 1337.

Figure 3. Partial 2D-TOCSY (400 MHz, 15 °C, C$_6$D$_5$CD$_3$, t_{mix} = 100 ms) of a solution containing 60% of d_{48}-**5**⊙**3b**. Cross-peaks between protons of **3b** are labeled.

J = 9.2 Hz), and 5.18 (d, 1H, J = 9.2 Hz), respectively. The methyl protons H6 are assigned to the singlet at δ −1.41 (3H) (Table 2).
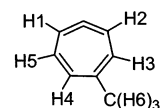
The assignment is supported via the observation of NOEs between H4 and H5 (strong), H2 and H3 (medium), H4 and

Table 1. Relative Product Yields (%)[a] for the Inner Phase Photolysis of **5⊙6** and d_{48}-**5⊙6**

entry	temp/solvent	hemicarceplex	5⊙3b/d_{48}-5⊙3b	5⊙12	14/d_{48}-14	15/d_{48}-15	16/d_{48}-16	17/d_{48}-17
1	273 K/CDCl$_3$[b]	**5⊙6**		81	6	4	6	
2	273 K/CDCl$_3$[c]	**5⊙6**			36	26		14
3	77 K/CDCl$_3$[c]	**5⊙6**			33	20	41	trace
4	77 K/C$_6$D$_5$CD$_3$[c]	**5⊙6**	41		41	<1	5	
5	77 K/C$_6$D$_5$CD$_3$[c]	d_{48}-**5⊙6**	67		5	2.5	10	

[a] Yields were determined from the integral of the singlet assigned to the methyl protons of each compound in the room temperature ^{1}H NMR spectra of the photolyzed solutions and are based on the amount of consumed **5⊙6**. [b] After 30 s of irradiation time at λ > 320 nm. [c] After prolonged irradiation at λ > 320 nm.

Table 2. Experimental (δ_{exp}) and Computed (δ_{calc}) ^{1}H NMR Chemical Shifts of **3b** and Calculated Host-Induced Upfield Shifts ($\Delta\delta$)[a]

|		B3LYP/6-311++(2d,p)		HF/6-311+(2d,p)	
	δ_{exp}	δ_{calc}	$\Delta\delta$	δ_{calc}	$\Delta\delta$
H1	2.58	6.00	3.42	5.78	3.36
H2	5.06	6.06	1.00	5.89	0.83
H3	4.65	6.34	1.69	6.08	1.43
H4	5.37	6.96	1.59	6.61	1.24
H5	5.18	6.51	1.33	6.31	1.13
H6	−1.41	2.28	3.69	2.00	3.41

[a] Calculations were performed on the B3LYP/6-311G* optimized geometry of **3b**.[14,20,21]

H6 (medium), and H3 and H6 (medium). Consistent with this assignment, cross correlation peaks are observed in the DQ-COSY spectrum of this solution between H4 and H5 and between H1 and H2. The calculated ^{1}H NMR chemical shifts of **3b** based on its B3LYP/6-311G* geometry using the DFT and HF approach together with the predicted hemicarcerand-induced shielding ($\Delta\delta$) are listed in Table 2 and suggest a guest orientation in which the methyl group is located in one of the host's cavitands, whereas the strained allene bond faces one of the aryl units of the opposite cavitand.[14,23,24]

Characterization of Innermolecular Tolylcarbene Insertion Products. We isolated four main *p*-tolylcarbene–hemicarcerand reaction products **14**–**17** and three of their deuterated derivatives d_{48}-**14**, d_{48}-**16**, and d_{48}-**17** by preparative thin-layer chromatography. Product **17** could only be obtained as a 4:1 mixture together with **15**. All products were characterized by ^{1}H NMR spectroscopy, elemental analysis, and mass spectrometry. The HR-MALDI MS and elemental analysis are consistent with reaction products resulting from insertion or addition of transient *p*-tolylcarbene to the surrounding host. The structures of these products were determined by 1D and 2D NMR experiments (DQCOSY, ROESY, and TOCSY) in combination with molecular mechanical calculations. We assign **14** and d_{48}-**14** to the products resulting from an insertion of transient **1b** into an inward-pointing acetal C–H bond of **5** and d_{48}-**5**,

respectively. Consistent with the C_s symmetry of **14**, the ^{1}H NMR spectrum shows a set of six chemically different outward-pointing acetal protons H$_o$ (ratio 1:1:1:1:2:2), six chemically different methine protons H$_m$ (ratio 1:1:1:1:2:2), and five chemically different inward-pointing acetal protons H$_i$ (ratio 1:1:1:2:2). The protons of the inner phase located *p*-methylbenzyl group are assigned to multiplets at δ 5.59 (d), 5.18 (d), 2.04 (m), and −0.60 (s) (Figure 4a, marked with arrows).

We assign **15** to a product resulting from the insertion of transient **1b** into a C–O bond of a host's 1,4-dioxybutane linker.[25] This insertion reaction creates a stereogenic center at the reacting carbon. Consistent with the C_1 symmetry of **15**, the ^{1}H NMR spectrum shows sets of eight chemically different protons for the aryl protons H$_a$, the outward-pointing acetal protons H$_o$, the inward-pointing acetal protons H$_i$, and the methine protons H$_m$, but only 15 chemically different linker α protons. The protons originating from reactant **1b** are assigned to multiplets at δ 6.19 (d, 2H), 5.86 (d, 2H), 3.88 (m, 1H), and −0.31 (s, 3H) (Figure 4b, marked with arrows).
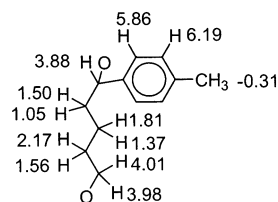
Both **16** and **17** are assigned to cyclopropanation products resulting from the addition of transient **1b** to an aryl unit of the surrounding host. The ^{1}H NMR spectra of both addition products show sets of eight chemically different protons for the inward- (H$_i$) and outward-pointing acetal protons (H$_o$) and the methine protons H$_m$. The tolyl protons of **16** are assigned to multiplets at δ 6.00 (d, 2H), 5.58 (d, 2H), and −1.38 (s, 3H), and those of **17** are assigned to multiplets at δ 6.35 (d, 2H), 5.88 (d, 2H), and −1.07 (s, 3H). The most characteristic features in the ^{1}H NMR spectra, which are consistent with aryl addition products, are the observation of only seven cavitand aryl protons H$_a$ in the expected chemical shift range between δ 7.0 and 6.6 in addition to two further upfield shifted singlets at δ 5.95 and −0.69 for **16** and at δ 5.25 and 3.08 for **17**, each integrating for one proton (Figure 4 c,d, marked with ● and ▼). We assign both singlets to the vinyl proton H$_v$(**16**) (δ 5.95) and H$_v$(**17**) (δ 5.25) and benzyl proton H$_b$(**16**) (δ -0.69) and H$_b$(**17**) (δ 3.08) of **16** and **17**, respectively (Scheme 6).

An approximately 1−1.5 ppm upfield shift for H$_v$ as compared to H$_a$ is expected and would be difficult to explain

(23) (a) Becke, A. D. *Phys. Rev.* **1988**, *38*, 3098. (b) Lee, C.; Yang, W. R.; Parr, G. *Phys. Rev. B* **1988**, *37*, 785. (c) Frisch, M. J.; Trucks, G. W.; Schlegel, H. B.; Scuseria, G. E.; Robb, M. A.; Cheeseman, J. R.; Zakrzewski, V. G.; Montgomery, J. A., Jr.; Stratmann, R. E.; Burant, J. C.; Dapprich, S.; Millam, J. M.; Daniels, A. D.; Kudin, K. N.; Strain, M. C.; Farkas, O.; Tomasi, J.; Barone, V.; Cossi, M.; Cammi, R.; Mennucci, B.; Pomelli, C.; Adamo, C.; Clifford, S.; Ochterski, J.; Petersson, G. A.; Ayala, P. Y.; Cui, Q.; Morokuma, K.; Malick, D. K.; Rabuck, A. D.; Raghavachari, K.; Foresman, J. B.; Cioslowski, J.; Ortiz, J. V.; Stefanov, B. B.; Liu, G.; Liashenko, A.; Piskorz, P.; Komaromi, I.; Gomperts, R.; Martin, R. L.; Fox, D. J.; Keith, T.; Al-Laham, M. A.; Peng, C. Y.; Nanayakkara, A.; Gonzalez, C.; Challacombe, M.; Gill, P. M. W.; Johnson, B. G.; Chen, W.; Wong, M. W.; Andres, J. L.; Head-Gordon, M.; Replogle, E. S.; Pople, J. A. *Gaussian 98*, revision A.7; Gaussian, Inc.: Pittsburgh, PA, 1998.
(24) (a) Becke, A. D. *J. Phys. Chem.* **1993**, *98*, 5648. (b) Lee, C.; Yang, W.; Parr, R. G. *Phys. Rev. B* **1988**, *37*, 785.

(25) (a) Frey, H. M.; Voisey, M. A. *J. Chem. Soc., Chem. Commun.* **1966**, 454. (b) Nozaki, H.; Takaya, H.; Noyori, R. *Tetrahedron* **1966**, *22*, 3393. (c) Tomioka, H.; Suzuki, S.; Izawa, Y. *Bull. Chem. Soc. Jpn.* **1982**, *55*, 492.
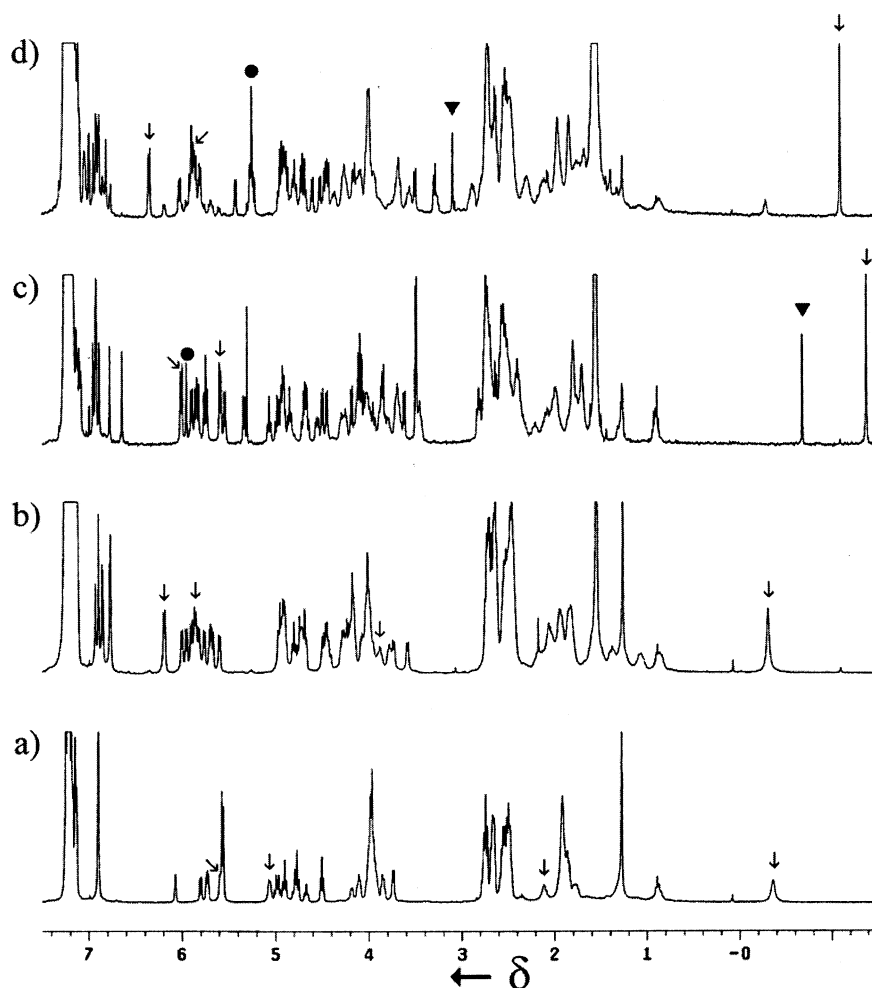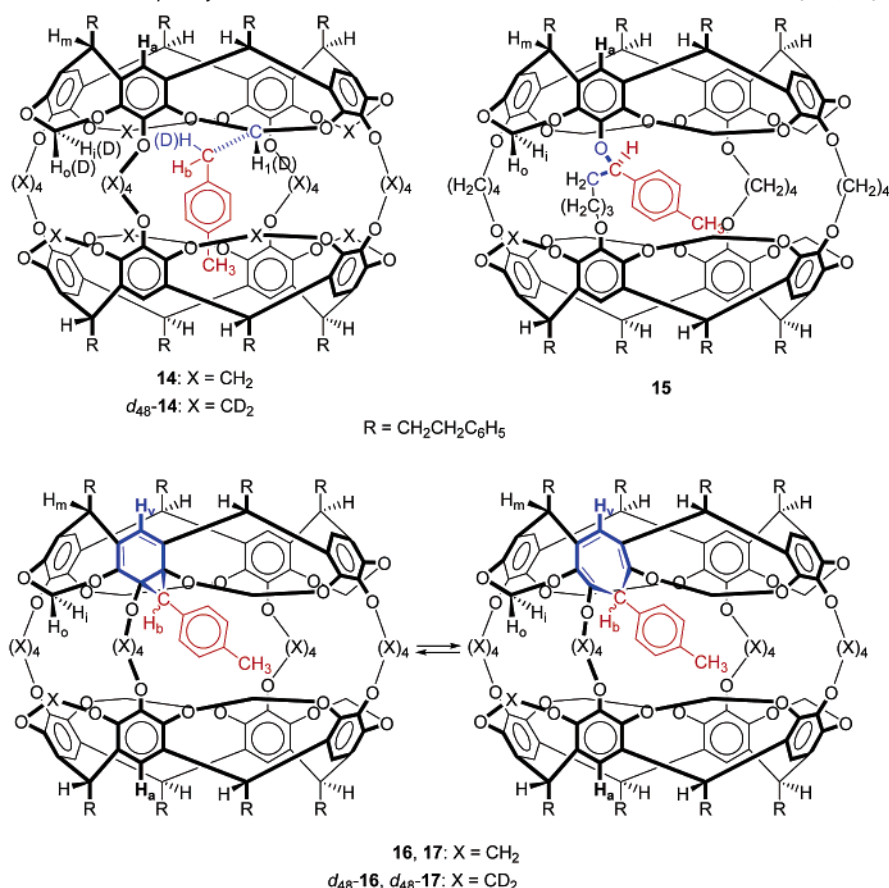
Figure 4. ^{1}H NMR spectra (400 MHz, CDCl$_3$, 23 °C) of innermolecular *p*-tolylcarbene reaction products **14** (a), **15** (b), **16** (c), and **17** (d). Spectrum d contains **17** and **15** in a 4:1 ratio. Multiplets assigned to the protons of the inner phase tolyl group are marked with arrows. Singlets assigned to the benzyl (H$_b$) and vinyl proton (H$_v$) of **16** and **17** are marked with a ▼ triangle (H$_b$) and a ●(H$_v$).

through other inner phase reactions of **1b**. For steric reasons, only the *p*-tolylcarbene addition to the C1−C2 (C2−C3) bond of a host's aryl unit seems possible. The addition of **1b** to the C1−C2 bond can lead to the *exo*- (*exo*-**NCD**) or *endo*-norcaradiene (*endo*-**NCD**), which could ring-open to the corresponding *exo*- (*exo*-**CHT**) or *endo*-cycloheptatrienes (*endo*-**CHT**). We carried out molecular mechanical calculations (MM3, vacuum) to get information about the structure and conformational energy of these compounds.[26] Molecular dynamics calculations (2 ns, 300 K) show that the average potential energy of the *endo*-isomers is lower than those of the *exo*-isomers. The final energy-minimized structures after 2 ns molecular dynamics runs are shown in Figure 5. In all products, the cyclopropanation induces a large distortion of the reacting cavitand such that even in *endo*-**NCD** and *exo*-**CHT** the 3,5-dioxacyclohepta-1,4-diene moiety closest to the reacting arene bond is in the boat rather than the chair conformation, which is usually observed in cavitands and hemicarcerands.[27] The negative and much smaller

(26) (a) Goodman, J. M.; Still, W. C. *J. Comput. Chem.* **1991**, *12*, 1110. (b) Allinger, N. L. *J. Am. Chem. Soc.* **1977**, *99*, 8127. (c) Still, W. C.; Tempczyk, A.; Hawley, R. C.; Hendrickson, T. *J. Am. Chem. Soc.* **1990**, *112*, 6127.
(27) (a) Houk, K. N.; Nakamura, K.; Sheu, C.; Keating, A. E. *Science* **1996**, *273*, 627. (b) Nakamura, K.; Houk, K. N. *J. Am. Chem. Soc.* **1995**, *117*, 1853. (c) Sheu, C.; Houk, K. N. *J. Am. Chem. Soc.* **1996**, *118*, 8056.

chemical shift of H$_b$(**16**) as compared to H$_b$(**17**) in combination with our molecular mechanical calculations suggests that **16** is an *exo*-isomer, in which H$_b$(**16**) deeply resides inside the strongly shielding inner cavity of the reacting cavitand. The same is true for the methyl protons, which are stronger shielded for **16** as compared to **17** consistent with the MM3 structures. In agreement with this assignment, the ROESY of **16** (t_{mix} = 600 ms) shows NOEs between H$_v$(**16**) and the CH$_2$ protons of the appending phenethyl groups at δ 2.79 (medium), 2.67 (medium), and 2.39 (strong), the two H$_a$ at δ 6.78 (weak) and 6.65 (weak) and H$_b$(**16**) (weak). Especially, the latter NOE (H$_v$(**16**) ↔ H$_b$(**16**)) cannot be explained with either one of the *endo*-isomers, in which the H$_b$−H$_v$ distances are greater than 5 Å. Consequently, we assign **17** to an *endo*-isomer. However, on the basis of our spectroscopic information, an unambiguous assignment of **16** and **17** to either a norcaradiene or a cycloheptatriene derivative is not possible. The following observations further support our assignment of **16** and **17** to arene/tolylcarbene addition products. (1) At room temperature in the solid state, **16** isomerizes very slowly to predominantly **17**. (2) The same isomerization can be induced photochemically. Brief irradiation of **5⊙6** at 0 °C yields **16** but not **17** (Table 1, entry 1 and Figure 1b). Further irradiation of the same solution slowly converts **16** into **17** (Table 1, entry 2 and Figure 1c). Even though the

Scheme 6. Structures of Four Isolated *p*-Tolylcarbenes−Hemicarcerand Reaction Products **14**−**17**, and d_{48}-**14**, d_{48}-**16**, and d_{48}-**17**[a]

14: X = CH₂
d_{48}-**14**: X = CD₂

15

R = CH₂CH₂C₆H₅

16, 17: X = CH₂
d_{48}-**16**, d_{48}-**17**: X = CD₂

[a] The atoms that originate from reactant **1b** are colored in red. The reacting C−H(D) or C−O bond, or aryl unit of **5**, is colored in blue.

isomerization mechanisms of **16** to **17** are not clear, they might involve **5⊙1b** as an intermediate.[28,29]

Thermal Rearrangements of 5⊙3b. In an effort to measure the barrier of the 5-methylcycloheptatetraene to *p*-tolylcarbene and *m*-tolylcarbene rearrangements, we investigated the thermal stability of d_{48}-**5⊙3b** by heating degassed solutions of d_{48}-**5⊙3b** in C₆D₅CD₃, which were sealed in NMR tubes, and recording periodically ¹H NMR spectra at room temperature. Heating the solution to 85 °C resulted in the slow decomposition of d_{48}-**5⊙3b** as determined from the decrease of the intensity of the singlet at δ −1.41 ppm, which is assigned to the methyl protons of **3b** (Figure 6). The thermolysis of d_{48}-**5⊙3b** followed first-order reaction kinetics in the experimental temperature range between 70 and 102 °C. Plots of $\ln([d_{48}$-**5⊙3b**$]_t/[d_{48}$-**5⊙3b**$]_{t=0})$ against time t gave straight lines (0.988 < r^2 < 0.998) (Figure 7), from which we determined the first-order rate constants k (Table 3).

Mechanistic considerations suggest that **3b** can rearrange to *m*-tolylcarbene **18** and to *p*-tolylcarbene **1b**. Recent calculations by Geise and Hadad predict essentially identical activation barriers for the rearrangement of **3b** to **1b** and **3b** to **18**,
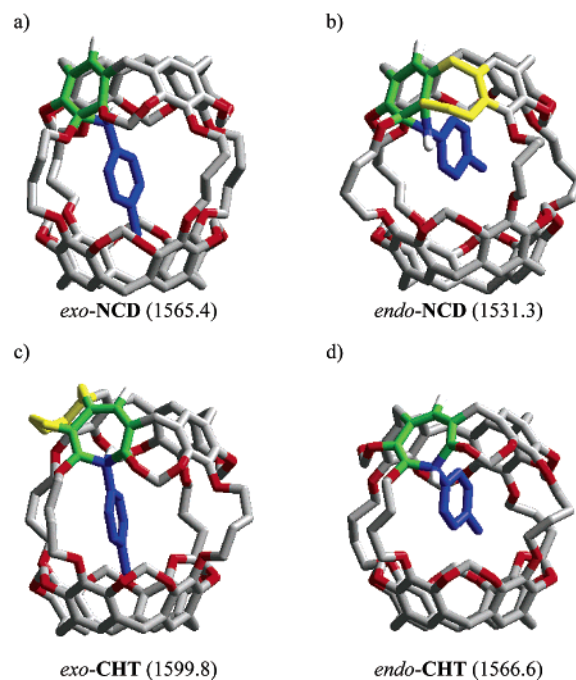
(28) (a) Klärner, F.-G. *Angew. Chem., Int. Ed. Engl.* **1974**, *13*, 268. (b) Klärner, F.-G. *Top. Stereochem.* **1984**, *15*, 1. (c) Kless, A.; Nendel, M.; Wilsey, S.; Houk, K. N. *J. Am. Chem. Soc.* **1999**, *121*, 4524.

(29) (a) Griffin, G. W. *Angew. Chem., Int. Ed. Engl.* **1971**, *10*, 537; *Angew. Chem.* **1971**, *83*, 604. (b) Richardson, D. B.; Durrett, L. R.; Martin, J. M., Jr.; Putman, W. E.; Slaymaker, S. C.; Dvoretzky, I. *J. Am. Chem. Soc.* **1965**, *87*, 2765. (c) Toda, T.; Nitta, M.; Mukai, T. *Tetrahedron Lett.* **1969**, 4401. (d) Ruck, R. T.; Jones, M., Jr. *Tetrahedron Lett.* **1998**, *39*, 4433. (e) Nigam, M.; Platz, M. S.; Showalter, B. M.; Toscano, J. P.; Johnson, R.; Abbot, S. C.; Kirchhoff, M. M. *J. Am. Chem. Soc.* **1998**, *120*, 8055.

exo-**NCD** (1565.4)

endo-**NCD** (1531.3)

exo-**CHT** (1599.8)

endo-**CHT** (1566.6)

Figure 5. Final energy-minimized structures of molecular dynamics runs (MM3, vacuum, 300 K, 2 ns) of four *p*-tolylcarbene-aryl addition products *exo*-**NCD** (a), *endo*-**NCD** (b), *exo*-**CHT** (c), and *endo*-**CHT** (d) together with their average potential energies (in kcal/mol). Hydrogens, except for H$_v$ and H$_b$ (for assignment see Scheme 6), and phenethyl groups are omitted for clarity. The atoms originating from the reacting aryl unit are colored in green, those from **1b** are colored in blue, and those of the 3,5-dioxacyclo-hepta-1,4-diene moiety in the boat conformation are colored in yellow.

Figure 6. Relative change in concentration of the d_{48}-**5**⊙**3b** (◆), d_{48}-**16** (▲), and **A** (○) during the thermolysis of d_{48}-**5**⊙**3b** at 85 °C in $C_6D_5CD_3$.
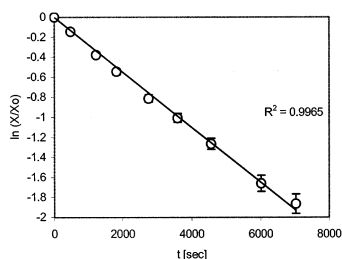
Figure 7. Plot of $\ln([d_{48}$-**5**⊙**3b**$]_t/[d_{48}$-**5**⊙**3b**$]_{t=0})$ against time t for the thermolysis of d_{48}-**5**⊙**3b** at 85 °C in $C_6D_5CD_3$.

Table 3. Rate Constants for the Thermal Decomposition of 5-Methylcycloheptatetraene (k), the 5-Methylcycloheptatetraene to p-Tolylcarbene Rearrangement (k_{p-TC}), and the 5-Methylcycloheptatetraene to p-Tolylcarbene Rearrangement (k_{m-TC}), and Initial p- to m-Tolylcarbene Ratio [**1b**]/[**18**] at Different Thermolysis Temperatures

T [°C]	k [10^{-4} s^{-1}]	[**1b**]/[**18**]	k_{p-TC} [10^{-4} s^{-1}]	k_{m-TC} [10^{-4} s^{-1}]
70.0	0.70 ± 0.06	0.65	0.27 ± 0.03	0.42 ± 0.04
77.8	1.5 ± 0.1	1.05	0.8 ± 0.06	0.7 ± 0.06
85.0	2.8 ± 0.2	1.28	1.5 ± 0.2	1.2 ± 0.1
89.1	4.4 ± 0.3	1.47	2.6 ± 0.2	1.7 ± 0.2
92.0	5.6 ± 0.3	1.39	3.2 ± 0.2	2.3 ± 0.2
97.2	9.5 ± 0.5	1.84	6.0 ± 0.4	3.3 ± 0.2
102.0	13.9 ± 0.6	1.93	8.9 ± 0.6	4.6 ± 0.3

Scheme 7
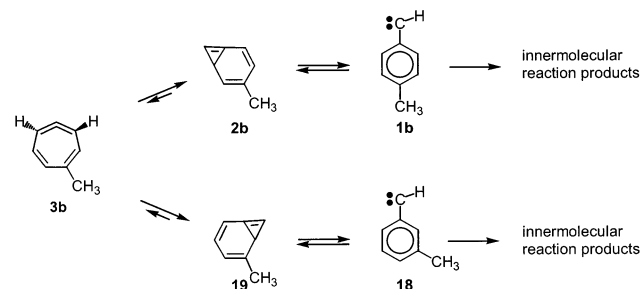
respectively.[8b] In the inner phase, transient **1b** and **18** will immediately react with the surrounding hemicarcerand to yield innermolecular reaction products (Scheme 7).

Alternatively, d_{48}-**5**⊙**3b** could decompose via dissociation leaving empty d_{48}-**5**, which will subsequently form d_{48}-**5**⊙$C_6D_5CD_3$. In this situation, the observed rate constant k is the sum of the rate constants for the **3b** to **1b** (k_{p-TC}) and **3b** to **18** (k_{m-TC}) rearrangements, and the dissociation of d_{48}-**5**⊙**3b** (k_{diss}), $k = k_{p-TC} + k_{m-TC} + k_{diss}$. Because **1b**, **18**, and empty d_{48}-**5** are formed from the same precursor, the rate constant of each decomposition channel of d_{48}-**5**⊙**3b** can be calculated from the amount of product formed in the particular reaction channel relative to the sum of all products.

In our product analysis, we proceeded as follows. Each tolylcarbene−hemicarcerand reaction product will have a strongly upfield shifted singlet ($\Delta\delta$ 1−4 pm) assigned to the methyl protons of the inner phase tolyl group. A spectral subtraction between ^{1}H NMR spectra recorded before and after heating the solution for 22.5 min to 85 °C showed an increase in the singlets assigned to the CH_3 and H_b protons of **16** (Figure 8). In addition, a second major product **A**, which is characterized by the two singlets at δ 0.99 and −0.74 (ratio 3:1) assigned to the methyl and the methine protons of its tolyl moiety, three further minor products **B**, **C**, and **D** with singlets for their methyl protons at δ −1.03, −1.48, and −1.36, and small amounts of d_{48}-**15** (approximately 1.5%) formed, but no C−D insertion of transient **1b** to yield d_{48}-**14** is observed. Product **D** formed also during the inner phase photolysis of **3b** and must be a p-tolylcarbene reaction product. The other three products **A**−**C** are new and are only observed if **3b** is used as the tolylcarbene precursor. Neither one is observed during the thermolysis of d_{48}-**5**⊙**6** or **5**⊙**6** under these conditions.[21] Therefore, we assign **A**, **B**, and **C** to m-tolylcarbene reaction products. Compound **A** is tentatively assigned to a product resulting from a cyclopropanation between **18** and an aryl unit of the surrounding hemicarcerand, similar to the formation of **16**.[30] The following facts provide support for our assignment. (a) Compound **A** is thermally fairly unstable. After an initial built up, it decomposes during the course of the thermolysis (Figure 6). This is not unexpected for a cyclopropanation product, whose formation we expect to be reversible.[31] (b) Simultaneously with the built-up of the two singlets at δ 0.99 and −0.74, multiplets at δ 6.3− 6.1 (2H), 4.27 (d, J = 7.0 Hz, 1H), and 2.90 (d, J = 1.9 Hz, 1H) built up (Figure 9a,b).[32] A 2D TOCSY spectrum of the thermolysis mixture, recorded at the point where **A** had built up to its maximum concentration, confirmed that both singlets and these multiplets belong to a common spin system. (c) The ROESY spectrum (t_{mix} = 1000 ms) of the same solution shows NOEs between the doublet at δ 4.28 and the singlet at d 0.99 and the multiplet at 6.18 (Figure 9c). Furthermore, NOEs are observed between the singlet at δ −0.74 and the doublet at 2.90 and the singlet at 0.99 and the doublet at 2.90, which is consistent with a m-methylbenzyl spin system.

Control experiments show that under these thermolysis conditions, approximately 3% of d_{48}-**5**⊙**3b** dissociates prior to the rearrangement of **3b**. Taking the amount of dissociation into account, the sum of assigned m- and p-tolylcarbene reaction products equals within the accuracy of integration the amount of decomposed d_{48}-**5**⊙**3b**. From k and the amount of m- and p-tolylcarbene products formed, we calculated k_{m-TC} and k_{p-TC} (Table 3). Arrhenius plots (Figure 10) provided activation parameters E_a and log A, from which we calculated $\Delta H^\ddagger$, $\Delta S^\ddagger$, and $\Delta G^\ddagger$, all listed in Table 4, together with the activation parameters calculated by Geise and Hadad using DFT calculations at the B3LYP/6-311+G** level of theory.[8b]

(30) Attempts to incarcerate m-tolyldiazirine inside hemicarcerand **5** to generate photochemically **18** inside **5** failed. We explain the failure with the poor shape match between m-tolyldiazirine and the inner phase of **5**.

(31) (a) Nefedow, O.; Nowizkaja, N.; Iwaschenko, A. *Liebigs Ann. Chem.* **1967**, *707*, 217. (b) Rautenstrauch, V.; Scholl, H.-J.; Vogel, E. *Angew. Chem., Int. Ed. Engl.* **1968**, *7*, 288; *Angew. Chem.* **1968**, *80*, 278. (c) Hoffmann, R. W.; Barth, W. *Chem. Ber.* **1985**, *118*, 634. (d) Vogel, E. *Pure Appl. Chem.* **1969**, *20*, 237. (e) Hoffmann, R. W. *Angew. Chem., Int. Ed. Engl.* **1971**, *10*, 529; *Angew. Chem.* **1971**, *83*, 595.

(32) The doublet at δ 4.31 (1H, J = 11.5 Hz) (Figure 9b) couples to the multiplet at δ 0.94 (dd, 1H, J = 11.5 Hz, 3.5 Hz) (Figure 8b) and is assigned to a methine proton H_m of **A**.
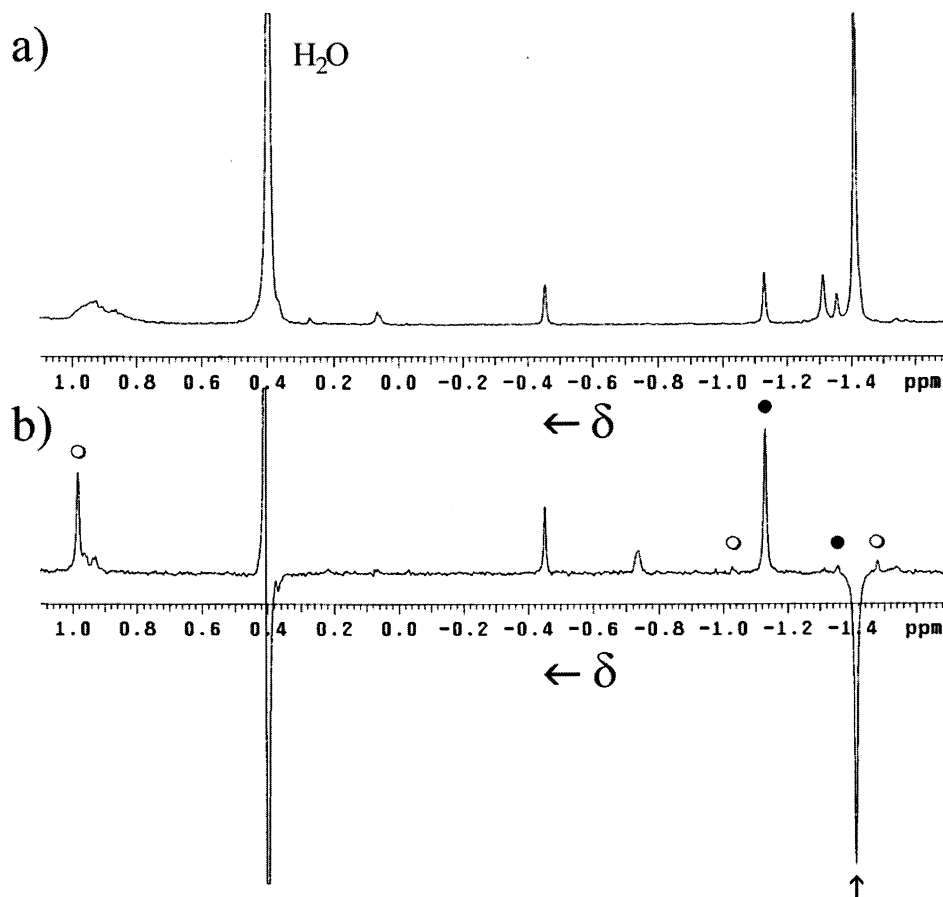
Figure 8. Partial ^{1}H NMR spectra (400 MHz, 23 °C, C$_6$D$_5$CD$_3$) of a solution containing 58% of d_{48}-**5**⊙**3b** (a) and spectral subtraction of ^{1}H NMR spectra after and before the solution was heated at 85 °C for 22.5 min (b). Signals that decrease or increase during the thermolysis are pointing downward and upward, respectively. Singlets assigned to the methyl protons of *m*-tolylcarbene products (**A**−**C**), *p*-tolylcarbene products (d_{48}-**16** and **D**), and **3b** are marked with ○, ●, and ↑, respectively.
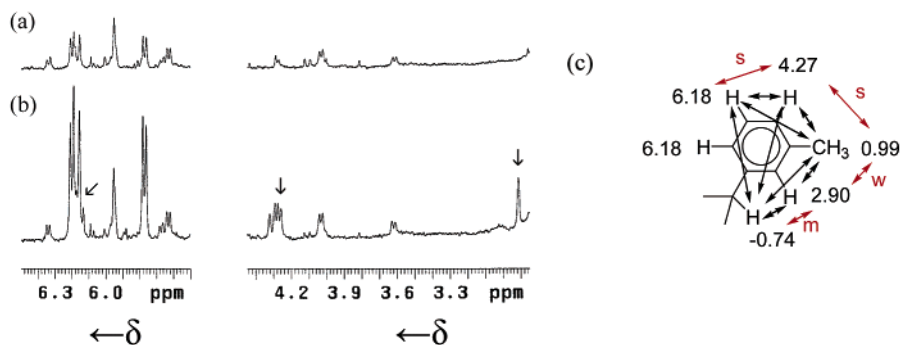

Figure 9. Partial ^{1}H NMR spectra (400 MHz, 23 °C, C$_6$D$_5$CD$_3$) of a solution containing 58% of d_{48}-**5**⊙**3b** after (b) and before (a) the solution was heated at 70 °C for 318 min. Multiplets assigned to the protons of inner phase tolyl group of **A** are indicated with arrows. (c) NOEs and TOCSY cross signals observed between the protons of the inner phase *m*-methylbenzyl moiety of compound **A**. NOEs are shown as red double headed arrows, and TOCSY cross correlations are indicated with black double-headed arrows; s, m, and w stand for strong, medium, and weak NOE, respectively.

If we compare the experimental with the ab initio activation parameters, we note (a) an excellent agreement between the measured and calculated activation free energies $\Delta G_{373}{}^{\ddagger}$ for the **3b** to **1b** rearrangement, but a slightly higher $\Delta G_{373}{}^{\ddagger}$ for the inner phase **3b** to **18** rearrangement. (b) Whereas $\Delta H_{373}{}^{\ddagger}$ and $\Delta S_{373}{}^{\ddagger}$ for the *p*-tolylcarbene rearrangement match very well, the measured and calculated activation enthalpies and entropies for the *m*-tolylcarbene rearrangement deviate strongly from each other. Similar enthalpy−entropy compensation effects are frequently observed in binding studies involving hemicarcerands or other hosts and are explained with a host and solvent

reorganization that accompanies the binding event.[33] We also attribute the observed enthalpy−entropy compensation in the *m*-tolylcarbene rearrangement to a reorganization of the hemicarcerand along the reaction coordinate and regard the fact that an enthalpy−entropy compensation of this magnitude is observed as indirect evidence for the intermediacy of 2-methylbicyclo[4.1.0]hepta-2,4,6-triene **19** in the **3b** to **18** rearrangement.

(33) (a) Grunwald, E. *Thermodynamics of Molecular Species*; Wiley-Interscience: New York, 1996. (b) Grunwald, E.; Steel, C. *J. Am. Chem. Soc.* **1995**, *117*, 5687. (c) Reichardt, C. *Solvents and Solvent Effects in Organic Chemistry*, 2nd ed.; VCH: Weinheim, 1988.
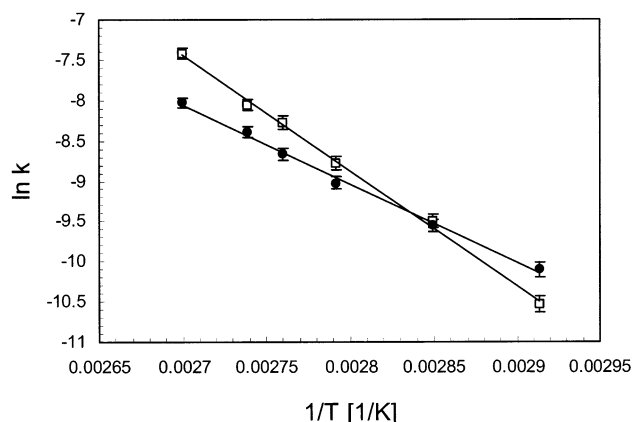
Figure 10. Arrhenius plot for the 5-methylcycloheptatetraene to *p*-tolylcarbene rearrangement ($\square$, $R^2 = 0.998$) and the 5-methylcycloheptatetraene to *m*-tolylcarbene rearrangement ($\bullet$, $R^2 = 0.998$).

Table 4. Experimental and Calculated Activation Parameters (in kcal/mol) for the 5-Methylcycloheptatetraene to *p*-Tolylcarbene Rearrangement and the 5-Methylcycloheptatetraene to *p*-Tolylcarbene Rearrangement[a]

reaction		E_a	log A	$\Delta H_{373}^{\ddagger}$	$-T\Delta S_{373}^{\ddagger}$	$\Delta G_{373}^{\ddagger}$	ref
$3b \rightarrow 1b$	exp.	27.2 ± 1.0	12.8 ± 0.6	26.4 ± 1.0	0.9 ± 1.0	27.3 ± 1.4	
	calc.			27.1	0.3	27.4	8b
	diff.[b]			-0.7	0.6	-0.1	
$3b \rightarrow 18$	exp.	20.5 ± 0.9	8.6 ± 0.6	19.7 ± 1.0	8.1 ± 1.0	27.8 ± 1.4	
	calc.			26.7	0.3	27.0	8b
	diff.[b]			-7.0	7.8	0.8	

[a] Standard errors were estimated by linear least squares regression of Arrhenius plots.[34] [b] Diff.: $\Delta H_{373}^{\ddagger}$(exp.) $- \Delta H_{373}^{\ddagger}$(calc.); $T\Delta S_{373}^{\ddagger}$(exp.) $- T\Delta S_{373}^{\ddagger}$(calc.); $\Delta G_{373}^{\ddagger}$(exp.) $- \Delta G_{373}^{\ddagger}$(calc.).

Discussion

Inner Phase Photochemistry of Tolyldiazirine. In previous work, we photolyzed phenyldiazirine inside hemicarcerand **5** or a partially deuterated host, which gave transient singlet phenylcarbene ^{1}**1a**.[15] The latter either inserted primarily into inward-pointing C−H (C−D) bonds of **5** or underwent intersystem crossing (ISC) to the ground-state triplet ^{3}**1a**. Below 77 K, ^{3}**1a** was long-lived enough to undergo photochemical ring-expansion to yield cycloheptatetraene **3a**. Photolysis of **6** inside the same host at 77 K gave 5-methylcycloheptatetraene **3b**. Our results support a mechanism for the photochemical generation of **3b** that is consistent with earlier work on the parent **3a** and with the matrix studies by Chapman and co-workers.[6] Incarcerated **6** primarily isomerizes photochemically to *p*-tolyldiazomethane **12**, which upon further photoexcitation yields singlet ^{1}**1b**. After intersystem crossing to the ground-state triplet ^{3}**1b**, the latter undergoes photochemical ring-expansion to **3b**. The yield of incarcerated **3b** depends strongly on the reaction temperature, the bulk phase, and the deuteration of the surrounding hemicarcerand. In particular, deuteration of the acetal spanners almost doubled the yield of **3b** as well as of all other competing reaction channels (formation of **15** and **16**). The reduced reactivity of ^{1}**1b** for C−D insertion increases the extent of ISC and produces more ^{3}**1b**. The much higher lifetime of ^{3}**1b**, for which we expect an even larger kinetic isotope effect as compared to that of ^{1}**1b**, strongly increases its probability to undergo a photochemical ring-expansion rather than an innermolecular reaction. In the liquid phase, **3b** was not observed. The failure to generate **3b** under these conditions excludes partial formation of **3b** via the direct ring-expansion of excited **6** or

12. At ambient temperature, **1b** is too short-lived and reacts with **5** prior to its photochemical excitation.

As compared to our earlier results on the inner phase phenylcarbene rearrangement, the yield in the photochemical tolylcarbene rearrangement is substantially higher. For example, photolysis of **5**⊙phenyldiazirine in $C_6D_5CD_3$ at 77 K gave less than 2% of **5**⊙**3a**,[15b] whereas 41% of **5**⊙**3b** is formed in the photolysis of **5**⊙**6** under the same conditions. This might be a consequence of the more restricted mobility of **1b** as compared to that of **1a**,[35] which prevents proper transition state geometries for innermolecular insertions into C−H and C−O bonds of **5**, and of the faster ISC rate of ^{1}**1b** as compared to that of ^{1}**1a**. Recent calculations by Geise and Hadad suggest an approximately 1.3 kcal/mol smaller singlet−triplet gap for **1b** as compared to **1a** due to the stabilization of the carbene p-orbital by the *p*-methyl substituent.[8a] The smaller singlet−triplet gap of **1b** may lead to a faster ISC to the ground state ^{3}**1b**.[36]

Interestingly, photolysis of **5**⊙**6** at 77 K in $CDCl_3$ failed to produce **5**⊙**3b** even though 41% of **5**⊙**3b** is formed in $C_6D_5CD_3$ as bulk solvent under these conditions. This is somewhat surprising in light of the recent discovery of a through-space heavy-atom effect that should increase the ISC rate constants of ^{1}**1b** in $CDCl_3$ to produce more ^{3}**1b** and consequently more **3b**.[37] Currently, it is not clear to us whether the shape of the inner phase and conformation of **5** are identical in frozen $CDCl_3$ and $C_6D_5CD_3$. A slight change of the conformation of **5** could change innermolecular reaction barriers and tunneling contributions and strongly decrease the lifetime of **5**⊙**1b** in $CDCl_3$. A more detailed study on the inner phase photochemistry of phenyldiazirine supports the view that the inner phase geometry strongly depends on the bulk phase.[35] Furthermore, at 77 K, $C_6D_5CD_3$ forms a transparent organic glass, whereas $CDCl_3$ is an amorphous solid that strongly scatters light. Even if more ^{3}**1b** is formed initially through a faster ISC of ^{1}**1b**, ^{3}**1b** and ^{1}**1b**, which are likely in a rapid spin equilibrium,[9a,38,39] might react with **5** prior to the excitation of ^{3}**1b**.

Inner Phase Kinetics of 5-Methylcycloheptatetraene. An important goal of our work was the investigation of the kinetics of 5-methylcycloheptatetraene. Upon heating d_{48}-**5**⊙**3b** in C_6D_5-CD_3 in the absence of oxygen, **3b** rearranged to **18** and **1b**, which subsequently reacted with the surrounding hemicarcerand to give predominantly cyclopropanation products d_{48}-**16** and **A**. This contrasts with its selectivity at low temperature. If we compare our measured activation parameters and those calculated by Geise and Hadad at the B3LYP//6-311+G** level of theory (Table 4), we note (1) a remarkable agreement between experimental and computed activation free energies $\Delta G_{373}^{\ddagger}$ for the **3b** to **1b** rearrangement and a slightly higher $\Delta G_{373}^{\ddagger}$ for the **3b** to **18** rearrangement in the inner phase. Earlier, we noted

(34) Bevington, P. R.; Robinson, D. K. *Data Reduction and Error Analysis for the Physical Sciences*, 2nd ed.; McGraw-Hill: New York, 1992; Chapter 6.
(35) Kemmis, C.; Warmuth, R. *J. Supramol. Chem.* **2002**, in press.
(36) Sitzmann, E. V.; Langan, J. G.; Griller, D.; Eisenthal, K. B. *Chem. Phys. Lett.* **1989**, *161*, 353.
(37) Romanova, Z. S.; Deshayes, K.; Piotrowiak, P. *J. Am. Chem. Soc.* **2001**, *123*, 2444.
(38) Moss, A. R.; Dolling, U.-H. *J. Am. Chem. Soc.* **1971**, *93*, 954.
(39) (a) Hadel, L. M.; Platz, M. S.; Scaiano, J. C. *Chem. Phys. Lett.* **1983**, *97*, 446. (b) Griller, D.; Hadel, L. M.; Nazran, A. S.; Platz, M. S.; Wong, P. C.; Savino, T. G.; Scaiano, J. C. *J. Am. Chem. Soc.* **1984**, *106*, 2227. (c) Griller, D.; Montgomery, C. R.; Scaiano, J. C. *J. Am. Chem. Soc.* **1982**, *104*, 6813. (d) Brauer, B.-E.; Grasse, P. B.; Kaufmann, K. J.; Schuster, G. B. *J. Am. Chem. Soc.* **1982**, *104*, 6814.

a similar excellent agreement between the inner phase and the computed activation free energy for the enantiomerization of **3b**.[14] We explain the small transition state destabilization in the inner phase *m*-tolylcarbene rearrangement with either the loss of attractive host−guest interactions (e.g., a C−H-π-interaction or a van der Waals contact) or the built-up of repulsive interactions due to steric constraints imposed by the surrounding hemicarcerand as the kinked transition state for the **19** to **18** isomeraion is reached. Consistent with the latter interpretation is the entropic nature of the activation free energy change. Steric interactions are more likely in inner phase reactions involving tight hemicarceplexes,[21] or if the reactant and/or transition state geometry strongly differ from the shape of the inner phase. (2) Whereas the calculated and experimental $\Delta H_{373}{}^{\ddagger}$ and $\Delta S_{373}{}^{\ddagger}$ for the **3b** to **1b** rearrangement are very similar, we observe a large enthalpy−entropy compensation effect in the **3b** to **18** rearrangement leading to a 7.0 kcal/mol smaller enthalpy contribution to $\Delta G_{373}{}^{\ddagger}$, which is compensated by a 7.8 kcal/mol larger entropy contribution ($-T\Delta S_{373}{}^{\ddagger}$). Large deviations between computed and measured activation enthalpies and entropies have been observed earlier for other rearrangements involving free carbenes in solution.[40] Even though the origin is not fully understood, limitations in the accuracy of the applied computational method have been suggested as a possible reason for these deviations. The structural similarity of the transition states for the *m*-tolylcarbene and *p*-tolylcarbene rearrangement makes an inaccuracy in the computed barriers a less likely reason for the observed enthalpy−entropy compensation in the *m*-tolylcarbene rearrangement. We rather believe that the surrounding host causes this compensation effect.

Enthalpy−Entropy Compensation in the 5-Methylcyclo-heptatetraene to *m*-Tolylcarbene Rearrangement. Enthalpy−entropy compensation effects are frequently observed in host−guest binding studies.[41−43] They are explained through a host and solvent reorganization that accompanies the binding event.[33,44] Host reorganization improves the fit between host and guest and strengthens the interactions between both (increase of $-\Delta H_{binding}$). This enthalpic gain is in part offset by an opposite entropy loss (increase of $-T\Delta S_{binding}$) due to the stiffening of the complex resulting in losses of degrees of freedom for host and guest. Usually the enthalpy−entropy compensation due to host reorganization is incomplete ($\Delta H > T\Delta S$), and the extent of compensation depends on the flexibility/rigidity of the host. However, solvent reorganization that accompanies a reaction or binding event leads to complete compensation.[33a,b] The favorable (disfavorable) enthalpy contribution to the free energy change resulting from an increased (decreased) solvation along the reaction coordinate is fully compensated by an equal entropy contribution as solvent is transferred from the bulk to the more ordered solvation sphere (or vice versa). The observation of an

Scheme 8
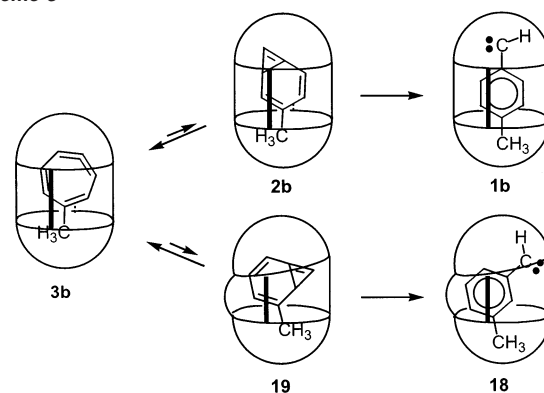
almost complete enthalpy−entropy compensation in the **3b** to **18** rearrangement and the absence of a strong compensation effect in the **3b** to **1b** rearrangement can be explained with similar host and solvent reorganizations.[15b] In the latter rearrangement, the shape of the guest does not change significantly along the reaction coordinate (**3b** → TS(**3b/2b**) → **2b** → TS(**2b/1b**) → **1b**). A host reorganization is not necessary or if it is, it will only be small. However, the shape of **18** and **19** differ strongly from that of **3b**. Therefore, in the **3b** to **18** rearrangement, we expect a host reorganization (e.g., bending) to compensate for the change in the guest shape, which could be accompanied by a solvent reorganization if the change in the solvent-exposed host surface is significantly large (Scheme 8). A hemicarcerand reorganization of this kind will likely take place on a much longer time scale as compared to the time scale of a single step chemical reaction.[45] This is an important point, and an enthalpy−entropy compensation of this magnitude should not be observed if the **3b** to **18** rearrangement would be a single step reaction. Hence, we regard the observation of an enthalpy−entropy compensation as indirect evidence for the intermediacy of **19** in the **3b** to **18** rearrangement.[7,8b,11,46] According to the ab initio calculations by Geise and Hadad, **19** is bound by $\Delta H_0 = 2.4$ kcal/mol.[8b] If we assume a normal Arrhenius preexponential factor, the lifetime of **19** at around 100 °C will be roughly 10 ps and long enough to allow a conformational change of **5** to tailor its inner phase to the kinked shape of **19**.

Conclusions

In the present and in an earlier investigation on the inner phase tolylcarbene rearrangement,[14] we have successfully measured the activation energies for the enantiomerization of the highly strained 5-methylcycloheptatetraene and its rearrangement to *m*- and *p*-tolylcarbene, which is an important part on the C_8H_8 potential energy surface. These barriers provide the first experimental support for the results of recent ab initio calculations.[8b] The excellent agreement between the inner phase activation barriers and those predicted at a high level of theory underlines that the inner phase of hemicarcerands is not only an excellent reaction environment to generate and stabilize highly strained reaction intermediates, but also allows an investigation of their dynamic behavior. Our investigations of

(40) (a) Albu, T. V.; Lynch, B. J.; Truhlar, D. G.; Goren, A. C.; Hrovat, D. V.; Borden, W. T.; Moss, R. A. *J. Phys. Chem. A* **2002**, *106*, 5323−5335. (b) Ho, G. J.; Krogh-Jespersen, K.; Moss, R. A.; Shen, S.; Sheridan, R. S.; Subramanian, R. *J. Am. Chem. Soc.* **1989**, *111*, 6875. (c) Moss, R. A.; Ho, G. J.; Shen, S.; Krogh-Jespersen, K. *J. Am. Chem. Soc.* **1990**, *112*, 1638.
(41) Piatnitski, E.; Flowers, R. A., II; Deshayes, K. *Chem.-Eur. J.* **2000**, *6*, 999.
(42) (a) Rekharsky, M.; Inoue, Y. *J. Am. Chem. Soc.* **2002**, *124*, 813. (b) Rekharsky, M.; Inoue, Y. *J. Am. Chem. Soc.* **2000**, *122*, 4418. (c) Inoue, Y.; Jiu, Y.; Tong, L.-H.; Shen, B.-J.; Jin, D.-S. *J. Am. Chem. Soc.* **1993**, *115*, 10637. (d) Inoue, Y.; Hakushi, T.; Jiu, Y.; Tong, L.-H.; Shen, B.-J.; Jin, D.-S. *J. Am. Chem. Soc.* **1993**, *115*, 475.
(43) Danil de Namor, A. F.; Ritt, M.-C.; Schwing-Weill, M.-J.; Arnaud-Neu, F.; Lewis, D. F. V. *J. Chem. Soc., Faraday Trans.* **1991**, *87*, 3231.
(44) Searle, M. S.; Westwell, M. S.; Williams, D. H. *J. Chem. Soc., Perkin Trans. 2* **1995**, 141.

(45) Cannon, W. R.; Benkovic, S. J. *J. Biol. Chem.* **1998**, *273*, 26257.
(46) If **3b** would rearrange via the σ-mechanism (single step), we would expect an incomplete compensation of any enthalpic transition state stabilization $\Delta\Delta H_{373}{}^{\ddagger} = \Delta H_{373}{}^{\ddagger}(\text{exp.}) - \Delta H_{373}{}^{\ddagger}(\text{calc.})$ by a loss in activation entropy ($-\Delta T\Delta S^{\ddagger}$) because the surrounding host would not reorganize within the time scale of the inner phase rearrangement.

the tolylcarbene rearrangement and of the thermal decomposition of aryldiazirines further show how the surrounding hemicarcerand modulates the reaction dynamics of incarcerated reactants and the heights of activation barriers.[21] Steric strain imposed on an inner phase transition state will increase the entropy contributions to $\Delta G^{\ddagger}$ simply by a stronger loss of vibrational degrees of freedom of the transition in the rather rigid inner phase as compared to the flexible solvent cage or the gas phase.[47] On the other hand, selective dispersion interactions between the transition state and the highly polarizable aryl units of the surrounding hemicarcerand tend to lower enthalpically $\Delta G^{\ddagger}$ by 2−3 kcal/mol.[21,48−50] Furthermore, enthalpy−entropy compensation effects are observed in multistep inner phase rearrangements, if an intermediate forms whose shape strongly differs from that of the reactant leading to a host and solvent reorganization that accompanies the reaction coordinate.[15b] In fact, the observation of a large enthalpy−entropy compensation effect in the **3b** to **18** rearrangement led us conclude that **19**, whose shape strongly differs from that of **3b**, is an intermediate in this rearrangement and that arylcarbenes rearrange via the π-mechanism (Scheme 2) as predicted from experiments by Miller and Gaspar (Scheme 4)[11] and from recent ab initio calculations.[7,8b] Nevertheless, our indirect evidence for **19** is weak, in part due to the difficulty in accurately measuring activation enthalpies and entropies and the lack of experimental activation parameters for the rearrangements of free **3b**. Thus, to fully settle the question of the bicyclo[4.1.0]hepta-2,4,6-triene participation in the phenylcarbene rearrangement, spectroscopic evidence would be desirable, which is a goal currently pursued in this laboratory.

Experimental Section

General. All reactions were conducted under argon unless otherwise noted. Tetrahydrofuran was freshly distilled from benzophenone ketyl just prior to use. HMPA was dried over activated molecular sieves (4 Å). DMF and NMP were purified by filtration through activated aluminum oxide and silica gel. ^{1}H NMR and ^{13}C NMR spectra were recorded on a 400 MHz Varian FT NMR spectrometer. Spectra taken in CDCl$_3$ or C$_6$D$_5$CD$_3$ were referenced to residual CHCl$_3$ or C$_6$D$_5$CD$_2$H at δ 7.26 and 2.09, respectively. FAB-MS were obtained on a ZAB SE instrument with a 3-nitrobenzyl alcohol matrix from the mass spectrometry laboratory at the University of Kansas, Lawrence, KS. HR-MALDI-TOF mass spectra were obtained on an Ion Spec HiRes-MALDI mass spectrometer. CHN elementary analyses were obtained from Desert Analytics, Tucson, AZ. Gravity chromatography was performed on Bodman silica gel (70-230 mesh). Thin-layer chromatography involved aluminum-backed plates (silica gel 60, F$_{254}$, 0.25 mm).

Hemicarceplex d_{48}-5⊙6. A suspension of d_{40}-**10** (150 mg; 0.067 mmol),[14] d_8-butane-1,4-diol dimesylate (0.135 g; 0.53 mmol, 8 equiv),[14] anhydrous cesium carbonate (0.7 g), and **6** (110 μL)[18] in dry HMPA (8 mL) was stirred under argon at room temperature in the dark for 5

(47) For other examples, see: (a) van Wageningen, A. M. A.; Timmerman, P.; van Duynhoven, J. P. M.; Verboom, W.; van Veggel, F. C. J. M.; Reinhoudt, D. N. *Chem.-Eur. J.* **1997**, *3*, 639. (b) Körner, S. K.; Tucci, F. C.; Rudkevich, D. M.; Heinz, T.; Rebek, J., Jr. *Chem.-Eur. J.* **2000**, *6*, 188.

(48) (a) McCurdy, A.; Jimenez, L.; Stauffer, D. A.; Dougherty, D. A. *J. Am. Chem. Soc.* **1992**, *114*, 10314. (b) Ngola, S. M.; Dougherty, D. A. *J. Org. Chem.* **1996**, *61*, 4355.

(49) Marquez, C.; Nau, W. M. *Angew. Chem., Int. Ed.* **2001**, *40*, 4387; *Angew. Chem.* **2001**, *113*, 4515.

(50) For examples of accelerations of bimolecular reactions, see: (a) Kang, J.; Rebek, J., Jr. *Nature* **1996**, *385*, 50. (b) Kang, J.; Santamaría, J.; Hilmersson, G.; Rebek, J., Jr. *J. Am. Chem. Soc.* **1998**, *120*, 7389. (c) Kang, J.; Hilmersson, G.; Santamaría, J.; Rebek, J., Jr. *J. Am. Chem. Soc.* **1998**, *120*, 3650. (c) Rebek, J., Jr.; Chen, J. *Org. Lett.* **2002**, *4*, 327.

days. The reaction mixture was pipetted into 40 mL of brine and filtered. The collected precipitate was washed with 2 × 5 mL water and 2 × 5 mL methanol and dissolved in CHCl$_3$ (10 mL). After the evaporation of the solvent, the residual crude product was dried under vacuum for 30 min. It was dissolved in the minimum amount of CHCl$_3$ and purified by column chromatography (SiO$_2$; eluant CHCl$_3$) to yield d_{48}-**5⊙6** as a white powder (110 mg; 60% yield). ^{1}H NMR (400 MHz; C$_6$D$_5$CD$_3$; 23 °C): δ 7.2−7.0 (m, 48H), 6.12, 6.08 (AB spin system, J_{AB} = 8.0 Hz, 4H, guest aryl), 5.22 (t, 4H, J = 7.6 Hz, CH$_{methine}$), 5.16 (t, 4H, J = 8.0 Hz, CH$_{methine}$), 2.70−2.60 (m, 16H, Ph−CH$_2$CH$_2$), 2.56−2.46 (m, 16H, Ph−CH$_2$CH$_2$), −1.48 (s, 1H, CH−methine, guest), −1.89 (s, 3H, CH$_3$, guest). FAB-MS (NBA-matrix): m/z 2430.2 ([M + 2]$^+$, 100%), 2400.7 ([M − N$_2$ + 2]$^+$, 78%), 2298.3 ([M − **6** + 2]$^+$, 45%).

Photolysis Experiments. General. In all photolysis experiments, samples were irradiated with the output of an Oriel 200 W Hg Power-Max lamp. A 10 cm water filter and a 320 nm cutoff filter (WG320) were placed between the lamp and the sample.

Sample Preparation. A solution of **5⊙6**[21] or d_{48}-**5⊙6** (2−3 mg) in toluene-d_8 or CDCl$_3$ (550 μL) was placed in a Pyrex NMR tube and was degassed by four freeze−pump−thaw cycles under vacuum. The NMR tube was sealed off under vacuum.

Photolysis at 77 K. Sample cooling was achieved with liquid nitrogen in a partially silvered dewar. The sample tube was placed in the light beam such that the bottom part of the frozen solution was in the focal point of the Power-Max lamp (4−5 mm diameter). First, the front of the sample was irradiated for 10 min, followed by a further 10 min irradiation after the sample tube had been turned by 180°. During this irradiation, the upper part of the frozen solution was protected from the light beam. After each 2 × 10 min irradiation period, the sample was moved downward in 5 mm steps until all of the frozen solution had been irradiated (typically 6−7 vertical steps). After the photolysis, all further sample manipulations were carried out using Schlenck line techniques.

Characterization of Photoproducts. p-Tolyldiazomethane Hemicarceplex 5⊙12. This was formed in 81% yield upon irradiating a degassed solution of **5⊙6** (3 mg) in CDCl$_3$ (0.6 mL) for 60 s at 0 °C. Characterization of crude product, ^{1}H NMR (400 MHz; CDCl$_3$; 22 °C): δ 7.25−7.15 (m, 40H), 6.88 (s, 8H), 5.94−5.86 (m, 2H, guest), 5.71 (sb, 8H), 4.89 (t, 8H, J = 8 Hz), 4.30 (sb, 4H), 4.20 (sb, 4H), 3.96 (sb, 8H), 3.87 (sb, 8H), 2.74−2.50 (m, 32H), 2.67 (s, 1H, guest), 1.81 (s, 16H), −1.76 (s, 3H, guest−CH$_3$). FT-IR (CHCl$_3$, 23 °C): v (cm^{-1}) 3005 (w), 2948 (m), 2876 (w), 2084 (m), 1517 (w), 1474 (s), 1454 (m), 1441 (s), 1374 (m), 1314 (s), 1155 (m), 1106 (m), 1065 (m), 1022 (m), 993 (s).

5-Methylcyclohepta-1,2,4,6-tetraene Hemicarceplex 5⊙3b. This was formed in 41% yield upon irradiating a degassed solution of **5⊙6** (3 mg) in C$_6$D$_5$CD$_3$ (0.55 mL) at 77 K as described above. Characterization of the crude product, ^{1}H NMR (400 MHz; C$_6$D$_5$CD$_3$; 23 °C): δ 7.2−7.0 (m, 48H), 5.73 (d, 8H, J = 7.2 Hz), 5.39 (d, 1H, J = 9.6 Hz guest), 5.2−5.0 (m, 11H), 4.65 (s, 1H), 4.45 (d, 8H, J = 7.2 Hz), 4.06−4.00 (m, 8H), 3.85 (t, 8H, J = 7.8 Hz), 2.75−2.40 (m, 33H), 1.81 (s, 8H), 1.78−1.72 (m, 8H), −1.42 (s, 3H, guest−CH$_3$).

5-Methylcyclohepta-1,2,4,6-tetraene Hemicarceplex d_{48}-5⊙3b. This was formed in 55−67% yield upon irradiating a degassed solution of d_{48}-**5⊙6** (3 mg) in C$_6$D$_5$CD$_3$ (0.55 mL) at 77 K as described above. Characterization of the crude product, ^{1}H NMR (400 MHz; C$_6$D$_5$CD$_3$; 23 °C): δ 7.2−7.0 (m, 48H, H_{aryl}), 5.38 (d, 1H, J = 9.5 Hz, guest), 5.17 (d, 1H, J = 9.5 Hz, guest), 5.15 (t, 8H, J = 7.9 Hz, CH$_{methine}$), 5.05 (d, 1H, J = 4.5 Hz, guest), 4.65 (s, 1H, guest), 2.75−2.40 (m, 32H, CH$_2$−CH$_2$−Ph), 2.58 (d, 1H, J = 4.5 Hz, guest), −1.41 (s, 3H, guest−CH$_3$).

p-Tolylcarbene−Hemicarcerand Insertion/Addition Products 14−17, d_{48}-14, d_{48}-16, and d_{48}-17. Purification of these photoproducts was achieved through preparative TLC on silica gel plates using CH$_2$Cl$_2$ as the mobile phase.

Acetal C−H Insertion Product (14). ^{1}H NMR (400 MHz; CDCl$_3$; 23 °C): δ 7.30−7.12 (m, 40H), 6.90 (s, 8H, aryl−H), 6.07 (t, 1H, J = 4 Hz, CH$_2$−CHOO), 5.80 (d, 1H, J = 6.8 Hz, OCHH_{outer}O), 5.73 (d, 1H, J = 7.2 Hz, OCHH_{outer}O), 5.72 (d, 1H, J = 7.6 Hz, OCHH_{outer}O), 5.59 (d, 2H, J = 7.2 Hz, tolyl−H), 5.57 (d, 2H, J = 6.8 Hz, OCHH_{outer}O), 5.07 (d, 2H, J = 7.2 Hz, tolyl−H), 5.00 (t, 1H, J = 7.6 Hz, $H_{methine}$), 4.97 (t, 1H, J = 8.4 Hz, $H_{methine}$), 4.91 (t, 2H, J = 8 Hz, $H_{methine}$), 4.79 (t, 1H, J = 8 Hz, $H_{methine}$), 4.77 (t, 2H, J = 8 Hz, $H_{methine}$), 4.67 (t, 1H, J = 7.6 Hz, $H_{methine}$), 4.51 (d, 1H, J = 6.8 Hz, OCHH_{inner}O), 4.49 (d, 1H, J = 7.2 Hz, OCHH_{inner}O), 4.18 (d, 1H, J = 7.2 Hz, OCHH_{inner}O), 4.14−4.08 (m, 2H, O−CH$_2$−CH$_2$), 4.05−3.90 (m, 12H, O−CH$_2$−CH$_2$), 4.00 (d, 2H, J = 6.8 Hz, OCHH_{inner}O), 3.88−3.81 (m, 2H, O−CH$_2$−CH$_2$), 3.74 (d, 2H, J = 6.8 Hz, OCHH_{inner}O), 2.80−2.45 (m, 32H, CH$_2$CH$_2$Ph), 2.12 (sb, 2H, tolyl−CH$_2$), 2.00−1.75 (m, 16H, OCH$_2$CH$_2$), −0.36 (sb, 3H, CH$_3$). HR-MALDI-TOF MS: [M + Na]$^+$, C$_{152}$H$_{144}$O$_{24}$Na calcd 2375.994; found 2376.006. Elemental analysis calcd (%) for C$_{152}$H$_{144}$O$_{24}$: C, 77.53; H, 6.17. Found: C, 77.58; H, 6.16.

d_{48}-Acetal C−H Insertion Product (d_{48}-14). ^{1}H NMR (400 MHz; CDCl$_3$; 23 °C): δ 7.30−7.12 (m, 40H), 6.90 (s, 8H, aryl−H), 5.59 (d, 2H, J = 8 Hz, tolyl−H), 5.08 (d, 2H, J = 8 Hz, tolyl−H), 4.99 (t, 1H, J = 7.6 Hz, $H_{methine}$), 4.97 (t, 1H, J = 8.4 Hz, $H_{methine}$), 4.91 (t, 2H, J = 7.2 Hz, $H_{methine}$), 4.79 (t, 1H, J = 8 Hz, $H_{methine}$), 4.77 (t, 2H, J = 8 Hz, $H_{methine}$), 4.67 (t, 1H, J = 7.6 Hz, $H_{methine}$), 2.80−2.44 (m, 32H, CH$_2$CH$_2$Ph), 2.12 (sb, 1H, tolyl−CHD), −0.36 (sb, 3H, CH$_3$). HR-MALDI-TOF MS: [M + Na]$^+$, C$_{152}$H$_{96}$D$_{48}$O$_{24}$Na calcd 2424.290; found 2424.297.

C−O Insertion Product (15). ^{1}H NMR (400 MHz; CDCl$_3$; 23 °C): δ 7.25−7.10 (m, 40H), 6.93 (s, 1H, aryl−H), 6.90 (s, 2H, aryl−H), 6.86 (s, 1H, aryl−H), 6.85 (s, 1H, aryl−H), 6.78 (s, 1H, aryl−H), 6.77 (s, 2H, aryl−H), 6.19 (d, 2H, J = 6.8 Hz, tolyl−H), 6.00 (d, 1H, J = 6.8 Hz, OCHH_{outer}O), 5.95 (d, 1H, J = 7.0 Hz, OCHH_{outer}O), 5.90 (d, 1H, J = 6.8 Hz, OCHH_{outer}O), 5.86 (d, 2H, J = 6.8 Hz, tolyl−H), 5.82 (d, 1H, J = 6.4 Hz, OCHH_{outer}O), 5.76 (d, 1H, J = 6.4 Hz, OCHH_{outer}O), 5.70 (d, 1H, J = 6.8 Hz, OCHH_{outer}O), 5.67 (d, 1H, J = 6.8 Hz, OCHH_{outer}O), 5.60 (d, 1H, J = 6.6 Hz, OCHH_{outer}O), 5.00 (t, 1H, J = 7.6 Hz, $H_{methine}$), 4.96 (d, 1H, J = 6.4 Hz, OCHH_{inner}O), 4.96 (t, 1H, J = 8.0 Hz, $H_{methine}$), 4.92 (t, 1H, J = 8.0 Hz, $H_{methine}$), 4.91 (t, 1H, J = 8.0 Hz, $H_{methine}$), 4.90 (t, 1H, J = 8.0 Hz, $H_{methine}$), 4.80 (t, 1H, J = 8.0 Hz, $H_{methine}$), 4.76 (t, 1H, J = 8.0 Hz, $H_{methine}$), 4.74 (t, 1H, J = 8.0 Hz, $H_{methine}$), 4.73 (d, 1H, J = 6.8 Hz, OCHH_{inner}O), 4.69 (t, 1H, J = 8.0 Hz, $H_{methine}$), 4.68 (t, 1H, J = 8.0 Hz, $H_{methine}$), 4.49 (d, 1H, J = 6.8 Hz, OCHH_{inner}O), 4.45 (d, 1H, J = 7.0 Hz, OCHH_{inner}O), 4.48−4.40 (m, 1H, O−CH$_2$−CH$_2$), 4.23 (d, 1H, J = 6.8 Hz, OCHH_{inner}O), 4.32−4.14 (m, 6H, O−CH$_2$−CH$_2$), 4.09−3.94 (m, 6H, O−CH$_2$−CH$_2$), 4.01 (d, 1H, J = 6.8 Hz, OCHH_{inner}O), 3.94−3.84 (m, 1H, O−C(Ph)H−CH$_2$), 3.81−3.74 (m, 1H, O−CH$_2$−CH$_2$), 3.73 (d, 1H, J = 6.6 Hz, OCHH_{inner}O), 3.59 (d, 1H, J = 6.6 Hz, OCHH_{inner}O), 2.80−2.40 (m, 32H, CH$_2$CH$_2$Ph), 2.22−1.76 (m, 14H, CH$_2$CH$_2$CH$_2$-CH$_2$), 1.60−1.53 (m, 1H, OCH(Ph)−CH$_2$CH$_2$CHH−CH$_2$O), 1.52−1.48 (m, 1H, OCH(Ph)−CHHCH$_2$CH$_2$−CH$_2$O), 1.40−1.34 (m, 1H, OCH-(Ph)−CH$_2$CHHCH$_2$CH$_2$O), 1.10−1.00 (m, 1H, OCH(Ph)−CHHCH$_2$-CH$_2$−CH$_2$O), −0.31 (sb, 3H, CH$_3$). HR-MALDI-TOF MS: [M + Na]$^+$, C$_{152}$H$_{144}$O$_{24}$Na calcd 2375.994; found 2376.007. Elemental analysis calcd (%) for C$_{152}$H$_{144}$O$_{24}$·3H$_2$O: C, 75.79; H, 6.03. Found: C, 75.68; H, 5.99.

Aryl Addition Product (16). ^{1}H NMR (400 MHz; CDCl$_3$; 23 °C): δ 7.28−7.08 (m, 40H), 6.96 (s, 1H, aryl−H), 6.93 (s, 1H, aryl−H), 6.93 (s, 1H, aryl−H), 6.91 (s, 1H, aryl−H), 6.89 (s, 1H, aryl−H), 6.78 (s, 1H, aryl−H), 6.65 (s, 1H, aryl−H), 6.00 (d, 2H, J = 8 Hz, tolyl−H), 5.95 (s, 1H, CH$_{vinyl}$), 5.89 (d, 1H, J = 7.0 Hz, OCHH_{outer}O), 5.85 (d, 1H, J = 7.2 Hz, OCHH_{outer}O), 5.82 (d, 1H, J = 6.8 Hz, OCHH_{outer}O), 5.75 (d, 1H, J = 7.6 Hz, OCHH_{outer}O), 5.73 (d, 1H, J = 7.4 Hz, OCHH_{outer}O), 5.58 (d, 2H, J = 8 Hz, tolyl−H), 5.54 (d, 1H, J = 6.6 Hz, OCHH_{outer}O), 5.33 (d, 1H, J = 7.2 Hz, OCHH_{outer}O), 5.07 (t, 1H, J = 7.6 Hz, $H_{methine}$), 4.98 (t, 1H, J = 7.6 Hz, $H_{methine}$), 4.94 (t, 1H, J = 8.4 Hz, $H_{methine}$), 4.93 (d, 1H, J = 6.8 Hz, OCHH_{outer}O), 4.91 (t, 1H, J = 7.8 Hz, $H_{methine}$), 4.85 (t, 1H, J = 8.0 Hz, $H_{methine}$), 4.70 (t, 1H, J = 8.0 Hz, $H_{methine}$), 4.67 (d, 1H, J = 7.6 Hz, OCHH_{inner}O), 4.66 (t, 1H, J = 8.4 Hz, $H_{methine}$), 4.55 (dd, 1H, J = 5.4, 9.4 Hz, $H_{methine}$), 4.49 (d, 1H, J = 6.6 Hz, OCHH_{inner}O), 4.45 (d, 1H, J = 7.0 Hz, OCHH_{inner}O), 4.32−4.20 (m, 2H, O−CH$_2$−CH$_2$), 4.18 (d, 1H, J = 7.4 Hz, OCHH_{inner}O), 4.12 (d, 1H, J = 7.2 Hz, OCHH_{inner}O), 4.10 (d, 1H, J = 6.8 Hz, OCHH_{inner}O), 3.84 (d, 1H, J = 6.8 Hz, OCHH_{inner}O), 3.62 (d, 1H, J = 7.2 Hz, OCHH_{inner}O), 4.16−3.62 (m, 12H, O−CH$_2$−CH$_2$), 3.48−3.41 (m, 2H, O−CH$_2$−CH$_2$), 2.80−1.60 (m, 48H, CH$_2$CH$_2$Ph, O−CH$_2$−CH$_2$), −0.69 (s, 1H, CH$_{cyclopropyl}$), −1.38 (s, 3H, CH$_3$). HR-MALDI-TOF MS: [M + Na]$^+$, C$_{152}$H$_{144}$O$_{24}$Na calcd 2375.994; found 2376.007. Elemental analysis calcd (%) for C$_{152}$H$_{144}$O$_{24}$: C, 77.53; H, 6.17. Found: C, 77.38; H, 6.16.

d_{48}-Aryl Addition Product (d_{48}-16). ^{1}H NMR (400 MHz; CDCl$_3$; 23 °C): δ 7.30−7.08 (m, 40H), 6.95 (s, 1H, aryl−H), 6.93 (s, 1H, aryl−H), 6.92 (s, 2H, aryl−H), 6.89 (s, 1H, aryl−H), 6.78 (s, 1H, aryl−H), 6.65 (s, 1H, aryl−H), 6.00 (d, 2H, J = 8 Hz, tolyl−H), 5.95 (s, 1H, CH$_{vinyl}$), 5.58 (d, 2H, J = 8 Hz, tolyl−H), 5.07 (t, 1H, J = 7.6 Hz, $H_{methine}$), 4.98 (t, 1H, J = 8 Hz, $H_{methine}$), 4.94 (t, 1H, J = 8 Hz, $H_{methine}$), 4.91 (t, 1H, J = 7.2 Hz, $H_{methine}$), 4.84 (t, 1H, J = 8.0 Hz, $H_{methine}$), 4.69 (t, 1H, J = 8.0 Hz, $H_{methine}$), 4.65 (t, 1H, J = 8 Hz, $H_{methine}$), 4.55 (dd, 1H, J = 5.4, 10 Hz, $H_{methine}$), 2.90−2.25 (m, 32H, CH$_2$CH$_2$Ph), −0.67 (s, 1H, CH$_{cyclopropyl}$), −1.39 (s, 3H, CH$_3$). HR-MALDI-TOF MS: [M + Na]$^+$, C$_{152}$H$_{96}$D$_{48}$O$_{24}$Na calcd 2424.290; found 2424.268.

Aryl Addition Product (17). This was isolated as a 4:1 mixture with the C−O insertion product 15. ^{1}H NMR (400 MHz; CDCl$_3$; 23 °C): δ 7.32−7.02 (m, 40H), 7.00 (s, 1H, aryl−H), 6.95 (s, 1H, aryl−H), 6.93 (s, 2H, aryl−H), 6.92 (s, 2H, aryl−H), 6.90 (s, 1H, aryl−H), 6.89 (s, 1H, aryl−H), 6.82 (s, 1H, aryl−H), 6.35 (d, 2H, J = 7.6 Hz, tolyl−H), 6.02 (d, 1H, J = 7.2 Hz, OCHH_{outer}O), 5.91 (d, 1H, J = 7.2 Hz, OCHH_{outer}O), 5.88 (d, 2H, J = 7.6 Hz, tolyl−H), 5.86 (d, 1H, J = 7.6 Hz, OCHH_{outer}O), 5.81 (d, 1H, J = 6.8 Hz, OCHH_{outer}O), 5.42 (d, 1H, J = 7.2 Hz, OCHH_{outer}O), 5.27 (d, 1H, J = 8 Hz, OCHH_{outer}O), 5.26 (d, 1H, J = 8 Hz, OCHH_{outer}O), 5.25 (s, 1H, CH$_{vinyl}$), 5.23 (d, 1H, J = 6.8 Hz, OCHH_{outer}O), 4.95 (t, 1H, J = 8 Hz, $H_{methine}$), 4.93 (t, 1H, J = 8 Hz, $H_{methine}$), 4.90 (t, 1H, J = 8 Hz, $H_{methine}$), 4.89 (t, 1H, J = 7.2 Hz, $H_{methine}$), 4.87 (d, 1H, J = 7.2 Hz, OCHH_{inner}O), 4.79 (t, 1H, J = 8 Hz, $H_{methine}$), 4.72 (d, 1H, J = 6.8 Hz, OCHH_{inner}O), 4.69 (t, 1H, J = 8 Hz, $H_{methine}$), 4.60 (d, 1H, J = 7.2 Hz, OCHH_{inner}O), 4.52 (d, 1H, J = 7.2 Hz, OCHH_{inner}O), 4.47 (d, 1H, J = 7.2 Hz, OCHH_{inner}O), 4.43 (d, 1H, J = 7.2 Hz, OCHH_{inner}O), 4.41−3.90 (m, 12H, OCH$_2$CH$_2$), 3.99 (t, 1H, J = 8 Hz, $H_{methine}$), 3.72−3.64 (m, 2H, OCH$_2$CH$_2$), 3.68 (t, 1H, J = 8.4 Hz, $H_{methine}$), 3.58−3.52 (m, 1H, OCH$_2$CH$_2$), 3.50 (d, 1H, J = 6.8 Hz, OCHH_{inner}O), 3.30−3.24 (m, 1H, OCH$_2$CH$_2$), 3.29 (d, 1H, J = 8 Hz, OCHH_{inner}O), 3.08 (s, 1H, CH$_{cyclopropyl}$), 2.94−2.40 (m, 32H, CH$_2$CH$_2$Ph), 2.38−1.60 (m, 16H, OCH$_2$CH$_2$), −1.07 (s, 3H, CH$_3$). HR-MALDI-TOF MS: [M + Na]$^+$, C$_{152}$H$_{144}$O$_{24}$Na calcd 2375.994; found 2375.995. Elemental analysis calcd (%) for C$_{152}$H$_{144}$O$_{24}$·CHCl$_3$: C, 74.27; H, 5.91. Found: C, 74.04; H, 5.97.

d_{48}-Aryl Addition Product (d_{48}-17). ^{1}H NMR (400 MHz; CDCl$_3$; 23 °C): δ 7.32−7.02 (m, 40H), 7.01 (s, 1H, aryl−H), 6.95 (s, 1H, aryl−H), 6.93 (s, 2H, aryl−H), 6.92 (s, 2H, aryl−H), 6.90 (s, 1H, aryl−H), 6.89 (s, 1H, aryl−H), 6.82 (s, 1H, aryl−H), 6.35 (d, 2H, J = 8.2 Hz, tolyl−H), 5.88 (d, 2H, J = 8.2 Hz, tolyl−H), 5.26 (s, 1H, CH$_{vinyl}$), 4.95 (t, 1H, J = 8.4 Hz, $H_{methine}$), 4.93 (t, 1H, J = 8 Hz, $H_{methine}$), 4.90 (t, 1H, J = 8 Hz, $H_{methine}$), 4.89 (t, 1H, J = 8 Hz, $H_{methine}$), 4.79 (t, 1H, J = 8.4 Hz, $H_{methine}$), 4.68 (t, 1H, J = 7.6 Hz, $H_{methine}$), 3.99 (t, 1H, J = 8 Hz, $H_{methine}$), 3.67 (t, 1H, J = 8.4 Hz, $H_{methine}$), 3.08 (s, 1H, CH$_{cyclopropyl}$), 2.92−2.05 (m, 32H, CH$_2$CH$_2$Ph), −1.07 (s, 3H, CH$_3$). HR-MALDI-TOF MS: [M + Na]$^+$, C$_{152}$H$_{96}$D$_{48}$O$_{24}$Na calcd 2424.290; found 2424.265.

Hemicarceplex d_{48}-5⊙C$_6$D$_5$CD$_3$. This was formed upon exposure of a solution containing d_{48}-5⊙3b at room temperature to oxygen. Isolation of d_{48}-5⊙C$_6$D$_5$CD$_3$ was achieved through preparative TLC on silica gel plates using CH$_2$Cl$_2$ as mobile phase. ^{1}H NMR (400 MHz;

CDCl$_3$; 23 °C): δ 7.25−7.15 (m, 40H), 6.93 (s, 8H), 5.84 (d, 2H, J = 7.8 Hz, guest−H), 5.66 (t, 2H, J = 7.8 Hz, guest−H), 4.85 (t, 8H, J = 8 Hz), 3.33 (t, 1H, J = 7.8 Hz, guest−H), 2.74−2.50 (m, 32H), −1.78 (s, 3H, guest−CH_3). HR-MALDI-TOF MS: [M + Na]$^+$, C$_{151}$H$_{144}$O$_{24}$-Na calcd 2412.290; found 2412.302.

Hemicarceplex 5⊙C$_6$H$_5$CH$_3$.[22] Hemicarcerand **5** (20 mg, 8.9 mmol)[51] was dissolved in toluene (2 mL). The solution was sealed in a Pyrex tube and heated at 150 °C for 3 days. After the solution had cooled to room temperature, the tube was opened, and the solution was concentrated at the rotavaporator. The crude hemicarceplex was purified by column chromatography (SiO$_2$/eluant: CHCl$_3$), which gave **5**⊙C$_6$H$_5$CH$_3$ as a white powder (18 mg; 86% yield). ^{1}H NMR (400 MHz; CDCl$_3$; 23 °C): δ 7.25−7.15 (m, 40H), 6.93 (s, 8H), 5.85 (d, 2H, J = 7.6 Hz, guest−H), 5.70−5.67 (m, 10H), 4.86 (t, 8H, J = 7.8 Hz), 4.14 (d, 8H, J = 7.1 Hz), 3.87 (s, 16H), 3.34 (t, 1H, J = 7.7 Hz, guest−H), 2.74−2.50 (m, 32H), 1.93 (s, 16H), −1.76 (s, 3H, guest−CH_3).

Thermolysis of d_{48}-5⊙3b. A degassed photolyzed solution of d_{48}-**5**⊙**6** in C$_6$D$_5$CD$_3$ which was sealed in a Pyrex NMR tube and which contained typically 55−67% of d_{48}-**5**⊙**3b** was heated in a constant-temperature bath for a given time and was cooled rapidly to room temperature by immersing it into a bucket full of water. The progress of the thermolysis was followed by ^{1}H NMR spectroscopy. Typically, 10−15 ^{1}H NMR spectra were recorded in each experiment. The amount of d_{48}-**5**⊙**3b** in the sample was determined from the integral of the singlet at δ −1.44 (integrated area from δ −1.41 to −1.47), which we assign to the methyl protons of incarcerated **3b**. The integral of the methylene protons of the appending phenethyl groups (integrated region from δ −2.80 to −2.20) served as internal standards during these measurements. After more than 90% of d_{48}-**5**⊙**3b** had been decomposed, the NMR tube was opened and exposed to oxygen for 3 h, after which all remaining d_{48}-**5**⊙**3b** had been converted to of d_{48}-**5**⊙ C$_6$H$_5$CH$_3$ and CO$_2$. The integral of the completely decomposed sample (integrated area form δ −1.41 to −1.47) was subtracted from the integrals of the methyl protons of **3b**.

Product Analysis. Product analysis was carried out through integration of selected multiplets in the ^{1}H NMR spectrum before and after brief thermolysis (conversion less than 20%). The amount of *p*-tolylcarbene reaction products and *m*-tolylcarbene reaction products relative to the amount of decomposed **3b** was determined from the increased integrals of the multiplets at δ 6.32 (d, 2H, d_{48}-**15**), 0.07 (sb, 3H, d_{48}-**14**), −0.44 (s, 1H, d_{48}-**16**), −1.31 (s, 3H, unidentified

p-tolylcarbene insertion product), and −1.36 (s, 3H, unidentified *p*-tolylcarbene insertion product) and at δ −0.74 (s, 1H, compound **A**), −1.03 (s, 3H, unidentified *m*-tolylcarbene insertion product), and −1.48 (s, 3H, unidentified *m*-tolylcarbene insertion product), relative to the decreased integration of the singlet at δ −1.41 (s, 3H, d_{48}-**5**⊙**3b**).

Determination of the Extent of 3b Escape During the Thermolysis of d_{48}-5⊙3b. A solution of d_{48}-**5**⊙**3b** in degassed in C$_6$D$_5$CD$_3$, which had been prepared as described above, was heated to 100 °C until the ^{1}H NMR spectrum of this solution indicated the complete decomposition of d_{48}-**5**⊙**3b**. The solvent was pumped off at high vacuum. The remaining solid was dissolved in toluene (0.5 mL) and heated in a sealed tube at 130 °C for 3 days. The solvent was pumped off under high vacuum, and the remaining solid was redissolved in CDCl$_3$. The ^{1}H NMR spectrum indicated approximately 3% of d_{48}-**5**⊙C$_6$H$_5$CH$_3$, which was formed via the dissociation of d_{48}-**5**⊙**3b**, leading to empty d_{48}-**5**, followed by the incarceration of C$_6$D$_5$CD$_3$ and C$_6$D$_5$CD$_3$ to C$_6$H$_5$CH$_3$ guest exchange during the heating of the thermolysis products in toluene. To check whether d_{48}-**5**⊙**6** contained trace amounts of empty d_{48}-**5**, a degassed solution of d_{48}-**5**⊙**6** in C$_6$D$_5$CD$_3$ was extensively photolyzed at room temperature until the ^{1}H NMR spectrum of this solution showed no d_{48}-**5**⊙**6** or d_{48}-**5**⊙**12** anymore. The solvent was pumped off at high vacuum, and the sample was dissolved in toluene. The sample tube was sealed and heated at 120 °C for 3 days. The solvent was pumped off again, and the remaining white solid was redissolved in CDCl$_3$. The absence of d_{48}-**5**⊙C$_6$H$_5$CH$_3$ in the ^{1}H NMR spectrum of this solution demonstrated that the used sample of d_{48}-**5**⊙**6** contained no empty d_{48}-**5**.

Supporting Information Available: ROESY, DQCOSY spectra of **14**−**17**, TOCSY spectrum of **15**, ^{1}H, ROESY, DQCOSY, and TOCSY NMR spectra of a solution containing 60% of d_{48}-**5**⊙**3b**, and ^{1}H NMR spectra of d_{48}-**14**, d_{48}-**16**, d_{48}-**17**, d_{48}-**5**⊙**6**, and d_{48}-**5**⊙**13** (PDF). This material is available free of charge via the Internet at http://pubs.acs.org.

JA027831K

(51) Robbins, T.; Knobler, C. B.; Bellew, D.; Cram, D. J. *J. Am. Chem. Soc.* **1994**, *116*, 111.